Sustainable Chemistry for the Environment 3 (2023) 100031

Contents lists available at ScienceDirect

Sustainable Chemistry for the Environment

journal homepage: www.editorialmanager.com/scenv

Detection of PFAS via surface-enhanced Raman scattering: Challenges and future perspectives

Bhavya M.B. [a], Novuhulu Rhakho [a], Satya Ranjan Jena [a], Sudesh Yadav [b], Ali Altaee [b,*], Manav Saxena [a], Akshaya K. Samal [a,*]

[a] Centre for Nano and Material Sciences, Jain University, Ramanagara, Bengaluru 562 112, Karnataka, India
[b] Centre for Green Technology, School of Civil and Environmental Engineering, University of Technology Sydney, 15 Broadway, NSW 2007, Australia

ARTICLE INFO

Keywords:
Per- and polyfluoroalkyl substances (PFAS)
Surface-enhanced Raman scattering (SERS)
Fluorescence
Emerging contaminants and metal nanoparticles

ABSTRACT

The upsurge in the alarm about the hazardous effects of one of the important emerging contaminants, Per- and polyfluoroalkyl substances (PFAS) are increasing in recent days. Due to the widespread use of PFAS in various fields, it has a high tendency to be accumulated in the environment and living entities. Due to the persistent and carcinogenic nature of PFAS, it is necessary to detect and remove them from the environment. Chromatographic techniques combined with mass spectrometry are the current conventional methods for PFAS detection. Some more methods like liquid chromatography, solid-phase extraction, solid-phase mass extraction, tandem mass spectrometry, optical, electrochemical, fluorescence-based sensors, biosensors, etc. are also implemented to detect PFAS. Even though these methods could detect perfluorooctane sulfonic acid (PFOS) and perfluorooctanoic acid (PFOA), the detection limits attained through these methods are unsatisfactory, and the detection of other PFAS has not been prioritized. Surface-enhanced Raman scattering (SERS) technique can be a great solution for the sensing of PFAS as it is highly sensitive, specific, and has a lot of potential in water research for the detection of contaminants. Due to the challenges associated with detecting PFAS using SERS, there is a limited amount of literature available on this topic. The reason behind this is the strong fluorescence nature of PFAS, and it is widely recognized that distinguishing fluorescence emission from Raman scattering is challenging due to their similar origins. In this perspective, causes for fluorescence in Raman scattering and the different ways to diminish the fluorescence are detailed in the later section. The article discusses the limitations of current PFAS sensors, advantages and limitations of fluorescence-based detection of PFAS in Raman scattering. The challenges related to the PFAS detection and possible solutions to resolve the issues have been focused. Further, an insightful discussion towards future research directions in this field has been provided.

1. Introduction

Per- and polyfluoroalkyl substances (PFAS) are artificial anthropogenic organofluorine chemicals made up of carbon-fluorine chains with attached functional groups, which give them surfactant properties [1]. PFAS are a cluster of nearly 4000 exceedingly fluorinated aliphatic compounds that are employed in a variety of applications. It is predicted that anthropogenic activities emit more than 10 million tonnes of harmful chemicals into aquatic habitats each year. PFAS owing to their high thermal and chemical stability have widespread application as industrial, chemicals in fire-retardant or firefighting foams, as well as in consumer goods such as adhesives and cosmetics [2,3]. The surfactant properties of PFAS make them water-soluble [4]. As a result, higher concentrations or non-permissible levels of PFAS are found in the environment. Unfortunately, the toxicity of these compounds has recently come to light because of increased environmental and health awareness [1]. PFAS cause several health issues, including preeclampsia, infertility, thyroid disease, and a decreased response to vaccines. Extreme or high-level of exposure to PFAS has links to lipid metabolism which can contribute to the development of dyslipidaemia. Therefore, scientists are working to improve detection and treatment techniques for PFAS at lower concentrations [1,5,6]. In recent years, perfluorooctanoic acid (PFOA) and perfluorooctane sulfonic acid (PFOS) are the two most commonly studied long-chain PFAS among the family of various PFAS. In the pollutant studies, both have been registered as emerging contaminants and are integrated into the list of persistent organic

* Corresponding authors.
E-mail addresses: Ali.Altaee@uts.edu.au (A. Altaee), s.akshaya@jainuniversity.ac.in (A.K. Samal).

https://doi.org/10.1016/j.scenv.2023.100031
Received 4 February 2023; Received in revised form 12 July 2023; Accepted 6 August 2023
Available online 7 August 2023

pollutants. Apart from inorganic anions, a group of organic anionic chemicals known as PFAS has gained a lot of attention in the last few decades. These organic pollutants are proven to be persistent in nature and pose a potential threat to humans, aquatics, and the environment. PFAS are found to be the key constituents of aqueous film-forming foams, which act as oxygen suppressing surfactants and are generally used in firefighting [7,8]. The extensive use in firefighting as well as the discharges from ammonium perfluorooctanoate, fluoropolymer manufacture, and fluoropolymer dispersion have led to wide dispersal which also persists in the environment due to its inert fluorocarbon skeleton [9–11]. Hence, the advancement in development of exceptional sensor materials for the detection of PFAS has received special attention [12]. Fig. 1 shows the pictorial representation of diverse effects of PFAS on human health (male and female individually) [13].

The United States Environmental Protection Agency (USEPA) allotted "Drinking Water Health Advisories for PFOA and PFOS" at 70 parts per trillion (ppt) in 2019, and later in 2022, USEPA set 0.004 and 0.02 ppt limits for PFOA and PFOS, respectively [1,14]. The detection of PFAS above the reporting threshold is associated with manufacturing units, wastewater plants, landfill leachate sites, and fire training areas [1,14]. As a result, a great concern has been raised on the detection of concentration of PFAS in contaminated water to ensure public health [15]. Chromatographic techniques combined with mass spectrometry are currently used in conventional methods 533, 537, and 537.1 [3, 16–18]. Branched and linear isomers of PFAS can be detected via the conventional method 533 with a 1.8–13% relative standard deviation in high fortification (80 ng/L) [17]. Methods 537 and 537.1 are further improved to meet data quality objectives based on liquid chromatography solid-phase extraction, and /tandem mass spectrometry [19,20]. These methods are approved and validated by the USEPA. Nevertheless, real-time monitoring and on-field testing are difficult using these gold-standard methods. Further, Ryu et al. reviewed optical-based techniques and electrochemical-based sensors for PFAS detection [21]. The authors suggested to custom covalent organic frameworks (COF) to prepare sensing probes. Also, selectivity can be enhanced when target molecules form intermolecular hydrogen bonds with a sensing probe. Most recently, Menger et al. presented the challenges in sensor development and commercialization [19].

Table 1 provides an overview of the existing conventional analytical techniques for measuring PFAS in different environmental conditions.

The existing conventional analytical techniques for measuring PFAS in various environmental matrices include [22–32]:

Table 1
Existing conventional analytical techniques for measuring PFAS in different environmental matrices (sample), analytical tools, and respective limit of detection (LOD).

Sl No.	Sample	Analytical tool	LOD	Reference
1	River water and coastal wastewater	SPE-HPLC-MS/MS	0.05–0.22 ng/L	[23]
2	Ultrapure/ Deionized (DI) water	HPLC-MS/MS	0.01–12.3 μg/L 0.20–53.6 μg/L	[24]
3	DI water and artificial groundwater	LC-MS/MS	10–20 ng/L	[25]
4	Artificial groundwater (soil)	LC-MS/MS	0.02–0.5 ng/g	[26]
5	DI water	HPLC	1 mg/L	[27]
6	Water: methanol (1:4)	UPLC-MS	0.4 ng/mL	[28]
7	DI water	HPLC	0.11–0.18 mg/L	[29]
8	Tap water, river water, and well water	VALLME^s-LC-MS	1.6 ng/L	[30]
9	Biosolids and biosolid-amended soils	LC-MS/MS	0.02–0.5 ng/g	[31]
10	Groundwater, lake water, and river water	SPE-LC-MS/MS	0.1–1.0 ng/L	[32]

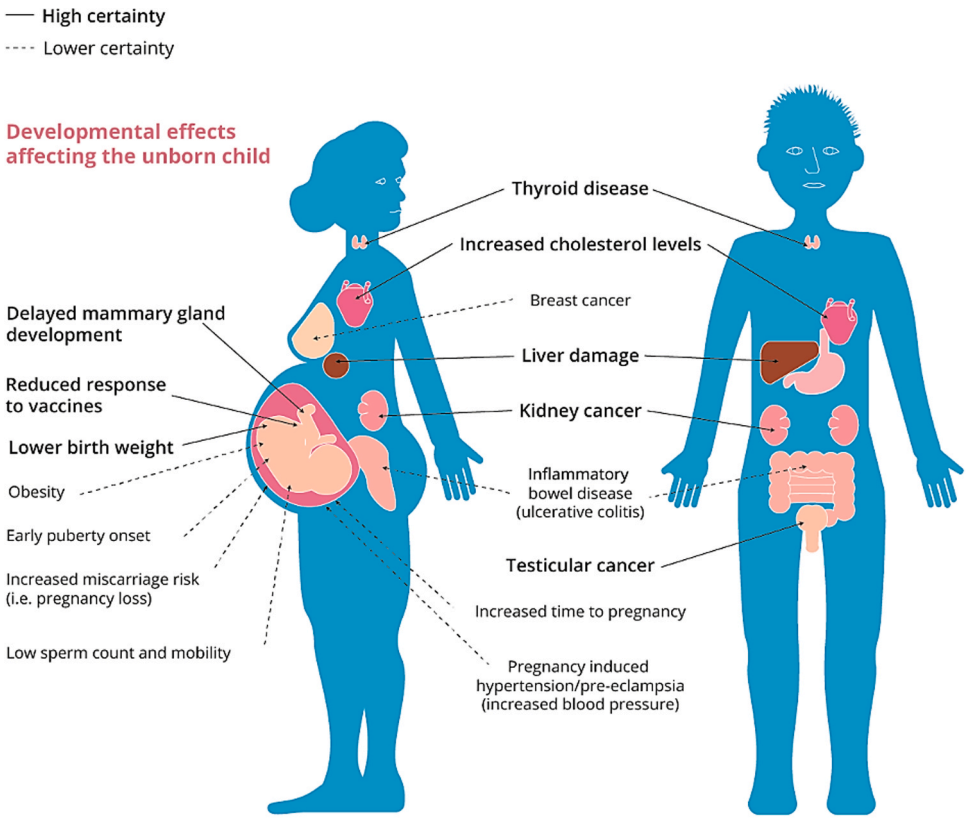

Fig. 1. Pictorial representation of diverse effects on human health (female & male) due to the existence of PFAS [13].

1. High-Performance Liquid Chromatography coupled with Tandem Mass Spectrometry (HPLC-MS/MS): This is the most common technique used for PFAS analysis. The process involves the separation of PFAS compounds using liquid chromatography, followed by their detection and quantification using tandem mass spectrometry.
2. Gas Chromatography-Mass Spectrometry (GC-MS): GC-MS is occasionally employed for analysing specific PFAS compounds. It involves separating PFAS compounds using gas chromatography after which they are detected and quantified using mass spectrometry.
3. Liquid Chromatography-Mass Spectrometry (LC-MS): LC-MS is another method used for analysing selected PFAS compounds. It involves separating PFAS compounds using liquid chromatography followed by the detection and quantifying them using mass spectrometry.
4. Orbitrap or Time-of-Flight (ToF) Mass Spectrometry**:** This method utilizes orbitrap or ToF MS for both qualitative and quantitative analysis of PFAS compounds in some cases. The other techniques include are,
5. SPE-HPLC-MS/MS - Solid Phase Extraction (SPE) coupled with High-Performance Liquid Chromatography (HPLC) and Tandem Mass Spectrometry (MS/MS)
6. UPLC-MS - Ultra-Performance Liquid Chromatography-Mass Spectrometry
7. SPE-LC-MS/MS - Solid Phase Extraction-Liquid Chromatography-Mass Spectrometry
8. VALLME^{s}-LC-MS- Vacuum-Assisted Liquid-Liquid Microextraction-Liquid Chromatography-Mass Spectrometry

The choice of analytical tool depends on factors such as the specific PFAS compounds being targeted, the desired level of sensitivity, and the type of information required from the analysis [22–32].

1.1. Limitations of currently available methods

However, existing approaches in PFAS analyses suffer from a considerable loss in sensitivity which may arise due to the low fragmentation yield of PFAS. Toxicological information has suggested regulatory parameters for PFAS of less than 1 ng/L [33] which is below the limit of quantification of current techniques. Furthermore, these techniques are time-consuming and difficult to access. A major drawback is their limited ability to analyse only a small fraction of the numerous existing PFAS compounds that exist. The extensive number of PFAS variants poses a challenge for currently existing methods to accurately report the concentrations [34]. These limitations hinder the advancement of scientific understanding and investigation within an already restricted domain. Consequently, the advancement of PFAS research demands a supplementary sensitive sensing technique capable of estimating the concentration of all PFAS. The existing detection approaches are primarily targeted on the detection of precise PFAS, such as PFOS and PFOA.

Surface-enhanced Raman spectroscopy (SERS) offers several advantages over conventional Raman spectroscopy and other traditional methods, making it a powerful analytical technique in various fields. The advantages of SERS, including its high sensitivity, selectivity, stability, multiplexing capability, versatility, and non-destructive nature, make it a valuable tool for sensing [35–37]. This perspective is focused on the development of SERS sensor technology for PFAS detection. Initially, the detection mechanism and operation of SERS were discussed. Subsequently, it provides technological advancements and future research directions based on SERS sensors for PFAS detection are summarised.

2. SERS detection mechanism for PFAS

2.1. Why SERS?

SERS is a powerful technique that is widely used to significantly enhance the inelastic light scattering of molecules (by factors of up to 10^8 or even greater in some cases), allowing for single-molecule SERS upon adsorption onto the surface of noble metal nanoparticles (MNPs) such as Ag or Au in most of the cases. Raman, an inelastic scattering was discovered in 1928 and has since been widely used as a spectroscopic technique for chemical analysis, sensing, and imaging. Raman scattering is a relatively weak signal that occurs when photons interact with molecules in an inelastic manner. The critical feature of the Raman scattering technique is the importance of molecular specificity and selectivity, which enable the unique identification of analytes. However, the primary disadvantage of this technique is the small signal or low quantum yield of scattering [38]. In 1973, Fleischmann observed the incredible enhancement (10^4 to 10^6) in the Raman signal for pyridine as an analyte on a silver electrode; the effect of using MNPs as substrate in Raman analysis set a benchmark [39]. The high enhancement in signal intensity is because metallic nanostructures (MNS) aid in the enhancement of electromagnetic signals through the well-known surface plasmon excitation. This technique of using MNS in the Raman analysis to improve the signal intensity for analyte detection is named as SERS [40]. Since SERS enhances Raman scattering by several orders of magnitude, it has a significant impact on ultra-low detection of analytes, low laser intensity, short acquisition times, high specificity, selectivity, multiple analyte detection, as well as single-molecule detection [41,42]. However, when the substrate surface is filled with MNS, Raman scattering can be significantly enhanced because of an increased electromagnetic field at the surface of the metal caused by improved incident light absorption. SERS has been extensively studied for various applications, due to the amplification of the signals in multi-folds. Compared to other optical techniques, SERS has several advantages in handling and detecting multiple analytes in the reaction mixture [43,44]. SERS stands as a milestone in the detection of environmentally hazardous analytes [45,46]. A schematic representation of SERS, representing the effect of placement of analyte at a different position on Au NPs on signal intensity is shown in Fig. 2 [47].

The Raman spectrum is unique due to the variety of vibrational modes present in each molecule. SERS is dependent not only on the shape, size, and structure of MNPs but also on the distance between the analyte and the surface of the metal, the orientation of the particles, and their conformation. The strength of the interaction between the analyte molecule and the MNPs determines the signal enhancement. The Raman intensity varies according to the position of the analyte, as depicted in Fig. 2. At position 1, as the analyte (represented as a star in neon colour) is located outside the metal surface, there is an absence of electromagnetic charge transfer between the metal surface and the analyte, resulting in very poor or no Raman scattering. When the analyte is at

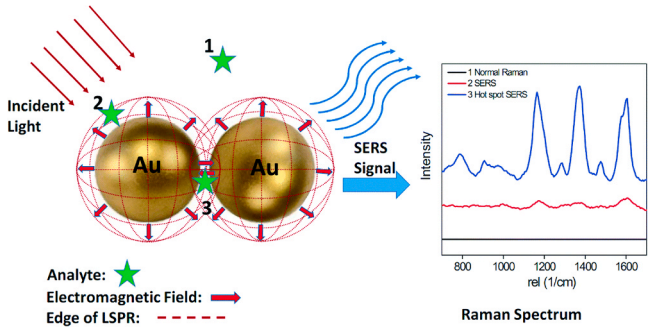

Fig. 2. Schematic illustration of SERS, representing the effect of placement of analyte at different positions on Au NPs with signal intensity [47].

position 2, an electromagnetic charge transfer is developed between the MNPs and the analyte, resulting in a weak Raman spectrum. Fig. 2 illustrates the weak Raman spectrum (red line spectrum) observed due to the presence of an analyte on the surface of the MNPs. When the analyte is present in between two MNPs, i.e., at the nanogaps (position 3 in Fig. 2), Raman scattering is enhanced. When the analyte is present at the nanogaps between the two metal surfaces, significant electromagnetic charge transfer occurs; as a result, a localized surface plasmon resonance (LSPR) effect is ascribed, increasing in Raman intensity, referred to as a hotspot. Raman scattering exhibits an extremely intense and sharp spectrum due to the presence of hotspot effects at the nanogaps (blue line spectrum). Clusters of two or more nanoparticles create an extinction range with multiple peaks, allowing for single-molecule detection via SERS. This effect is caused by the coupling of strong localized electromagnetic fields generated by incident light of appropriate wavelength and polarization on each nanoparticle. While electromagnetic field coupling decays exponentially with particle distance, it can exceed 2.5 times the diameter of the nanoparticle [43,48]. Fig. 3 shows the general schematic representation for the interaction of PFAS and sensor resulting in SERS signals.

The detection mechanism of analytes is generalized for PFAS using SERS, which involves several key factors [39–42,46,49]:

1. **Plasmonic Enhancement:** The detection sensitivity of PFAS is significantly enhanced in SERS due to the plasmonic enhancement effect. Plasmonic nanoparticles, typically made of Au or Ag, are used as the SERS substrate. These nanoparticles possess LSPR, which can enhance the electromagnetic field in their vicinity [50].
2. **Adsorption onto SERS Substrate:** PFAS molecules adsorb onto the surface of the plasmonic nanoparticles through various interactions, such as hydrogen bonding, electrostatic forces, and Van der Waals force of attraction. The adsorption facilitates the proximity of the analyte to the plasmonic surface, enhancing the Raman scattering signals [45,46].
3. **Electromagnetic Enhancement:** When the plasmonic nanoparticles are irradiated with a laser, the LSPR is excited, leading to an enhanced electromagnetic field in the vicinity of the nanoparticles. This enhanced electromagnetic field interacts with the adsorbed PFAS molecules, resulting in an increase in the Raman scattering signal intensity [51].
4. **Raman Signal Acquisition:** The incident laser excites the PFAS molecules, and as they return to their ground state, they emit Raman scattered light. The scattered light contains information about the vibrational modes and molecular structure of the PFAS molecules. The plasmonic enhancement amplifies the weak Raman signals, allowing for their detection and analysis [52].
5. **Specific Raman Fingerprints:** PFAS exhibit unique Raman spectra, which serve as their molecular "fingerprint". These spectra provide characteristic peaks corresponding to the specific vibrational modes of the PFAS molecules. By comparing the obtained Raman spectrum with reference spectra, the presence and identity of PFAS compounds can be determined [53].

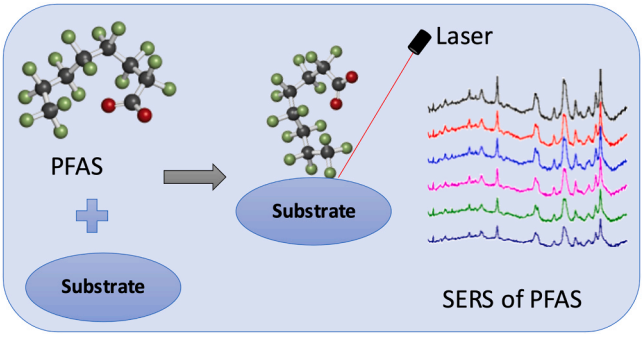

Fig. 3. Schematic representation for the interaction of PFAS and sensor resulting in SERS signals.

The combination of plasmonic enhancement, adsorption onto the SERS substrate, electromagnetic enhancement, and specific Raman fingerprints enables the sensitive detection and identification of PFAS using SERS. This technique offers advantages such as high sensitivity, selectivity, and the ability to analyse PFAS in complex matrices, making it a promising tool for PFAS analysis and monitoring.

2.2. *Detection mechanism*

Due to the excitation of LSPR attributed to MNPs, SERS significantly increases the intensity of Raman scattering from contaminants, which are adsorbed on or near the metallic surface. As a result, an ultrasensitive plasmon-enhanced spectroscopic method has been developed to retain Raman spectroscopy's intrinsic structural specificity while allowing experimental adaptability [54]. Thus, SERS is increasingly escalating into the arena of feasible environmental contaminant detection. SERS can significantly increase the Raman cross-section of a compound adsorbed on Au or Ag nanoparticles. SERS is triggered by two distinct mechanisms: electromagnetic enhancement (EE) and chemical enhancement (CE). The electromagnetic process occurs when involving an enhanced electromagnetic field near the nanoparticle's surface, nanogaps, and at the tips [55]. This enhancement occurred because of the MNPs' surface-amplification of electromagnetic radiation. CE, which includes metal-particles charge transfer (CT) to increase resonance with the Raman excitation laser, is less prominent. CE is highly dependent on the surface properties of the MNPs and the analyte molecule's nature [56]. Among both mechanisms, EE is considered as the main mechanism and CE occurs rarely [57,58].

The presence of EE and CE resulted in a multi-fold increase in the intensity of the SERS signal; however, the first EE is the primary contributor [59]. The EE is caused by the LSPR near the surface of noble MNPs. The EE mechanism in SERS is depicted in Fig. 4a, where I denotes the Raman intensity, E_i denotes the incident electric field, $E_{i,s}$ denotes the metal-induced field, and ($E_i + E_{i,s}$) denotes the incident enhanced field; Er denotes the scattered Raman field, which is intensified by the metal-induced $E_{r,s}$, and ($E_r + E_{r,s}$) denotes the scattered enhanced field [55]. CE, on the other hand, occurs because of electron transfer between the analyte substance and the nanomaterial surfaces when incident light energy collides with the energy associated with electron (Fig. 4b). This results in a change in molecular polarisation and a 10^2-fold increase in the Raman signal.

In Fig. 4b, three distinct CE mechanisms are illustrated: (i) CE of the ground state; (ii) Raman resonance enhancement; and (iii) charge-transfer resonance enhancement. In this figure, HOMO stands for the highest occupied molecular orbital, LUMO stands for the lowest unoccupied molecular orbital, and E_f stands for the local electromagnetic field. The total number of SERS enhancement features could theoretically reach 10^{14}, depending on the metallic nanostructure. Compared to the other two techniques, the EE technique exhibits a high degree of specificity and activity due to its high magnifying properties. When the CE technique is detected up to 10^2 times or more following the environmental conditions, the EE technique is detected up to 10^8 times or more in accordance with the environmental conditions [60,61].

At present, it is widely acknowledged that the primary factor contributing to the enhancement of the electromagnetic field (EF) is the electromagnetic mechanism (EM). This mechanism explains that the amplification of Raman signals takes place through surface plasmonresonance (SPR). In other words, when the energy of the laser used for excitation aligns closely with the surface plasmon energy of a substrate, typically composed of noble metal, the Raman response experiences significant enhancement. However, it is evident that there must be an additional mechanism to account for SERS results, which relies not only on the properties of the substrates but also on the characteristics of the

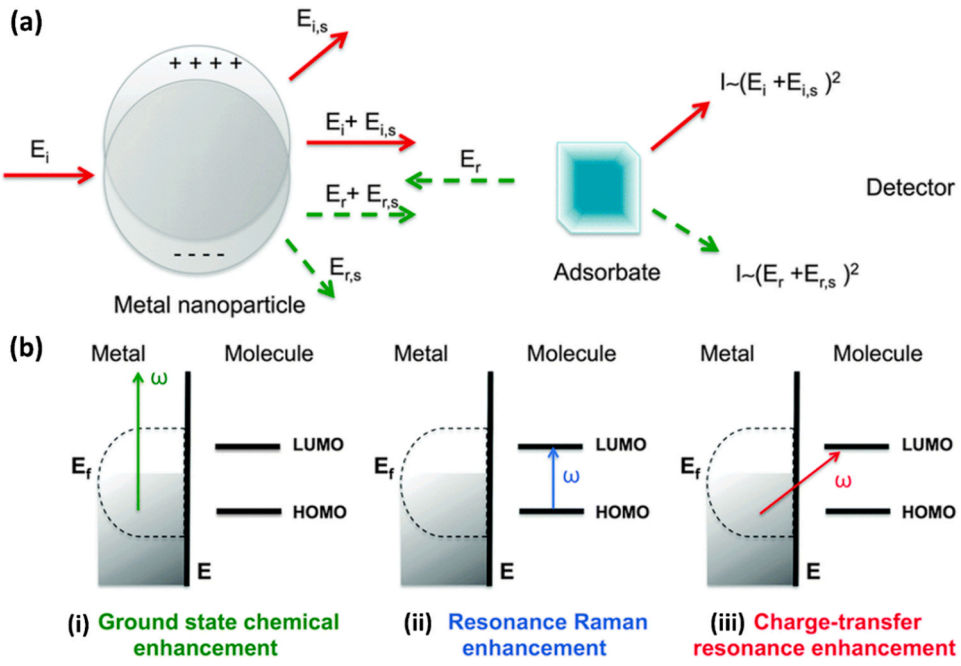

Fig. 4. Schematic illustration for the mechanism involved in SERS detection, (a) EC and (b) CE [55].

analyte molecules. This alternative mechanism is known as the chemical mechanism (CM). [62,63]. The term "CE" is a broad category rather than a specific phenomenon with a singular origin. It encompasses various transitions and processes. For instance, within a metal substrate, the most relevant aspect of CE is the CT transition between the HOMO of the analyte molecule and the Fermi level of the metal surface. In the case of dielectric substrates, the critical transitions involve charge transfer between either the HOMO of the molecule and the conduction band (CB)

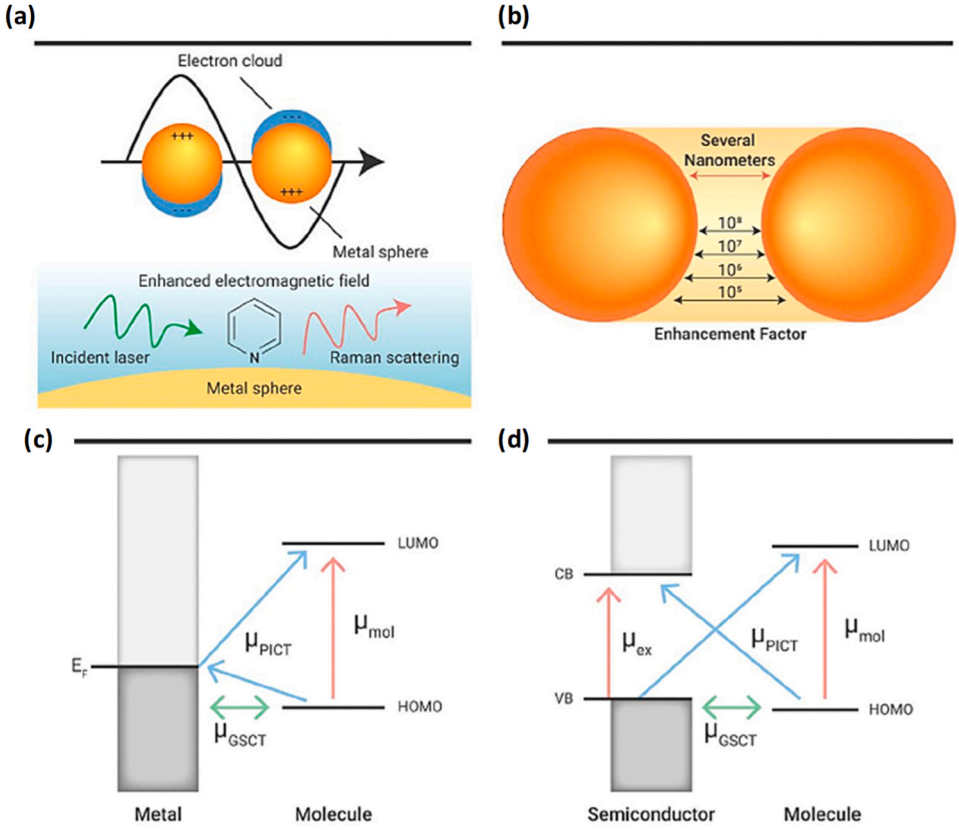

Fig. 5. Depicts an EM and CM for SERS enhancement. (a) Electromagnetic enhancement in plasmonic nanosphere-based SERS. (b) Representation of a "hot spot" in the space between adjacent particles and the accompanying change in SERS enhancement factor with relative positions. Charge-transfer transitions in a (c) metal-molecule system and (d) semiconductor-molecule system. [66].

edge of the substrate material, or the valence band (VB) of the substrate material and the LUMO of the molecules. Additionally, electronic transitions from HOMO to LUMO or transitions between the VB and CB of the substrate molecule could also add to the enhancement of Raman signals through resonance processes, leading to surface-enhanced resonance Raman spectroscopy (SERRS). All these effects can contribute to the enrichment of Raman results, and determining the exact origin of a specific enhancement is not always straightforward [64] While, the electromagnetic (EM) theory offers a satisfactory explanation for the underlying cause of enhanced Raman scattering, it struggles to account for the varying degrees of enhancement observed in different vibrational modes. To address this, a CM has been proposed, which suggests that CT occurring within the substrate molecule system can modify the electron density distribution of the molecules. This alteration leads to increased polarizability and, consequently, enhanced Raman scattering. Theoretically, the signal amplification achieved through the CM is estimated to range up to 10^3 for a hypothetical metal-molecular system.[65].

Fig. 5 demonstrates the EM and CM for SERS enhancement [66]. The initial stage involves a local field enhancement in the vicinity of the plasmonic nanoparticles at the incident frequency (ω_0), which is in resonance with the plasmon mode. This local field enhancement intensifies the Raman scattering process. The subsequent step involves an additional enhancement of the scattered Raman light when the Raman frequency (ω_R) coincides with the plasmon resonance, resulting in further amplification of the Raman signal (as illustrated in Fig. 5a). In theory, the maximum EE achievable in SERS conditions is approximately 10^{11}. However, this value can decrease significantly as the distance increases from the peak value observed at the shortest junction. Typically, the EM enhancement varies by orders of magnitude over small distances, such as a few molecular dimensions (approximately 2–4 nm).

In a collective theoretical and experimental study conducted by Petryayeva and Krull, they observed that the electromagnetic field exhibited a gap-size dependent behaviour [67]. Specifically, they found that the SERS enhancement increased from 10^5 to 10^9 as the gap amongst adjacent Au nanoparticles size reduced from 10 nm to 2 nm (as depicted in Fig. 5b). This demonstrates the significant impact of gap size on the enhancement of SERS signals. Jensen et al. introduced three different forms of CT contributions to elucidate the chemical impact in a metal-molecule system [68]. These include the transfer of ground-state charge at the interface (μ_{GSCT}), the photo-induced CT (μ_{PICT}), and the resonance of electronic excitation within the molecule itself. The schematics shown in Fig. 5c and d illustrate the three types of contributions to enhancements in SERS. Firstly, the enhancement resulting from ground-state CT (μ_{GSCT}) is a non-resonant effect, where the molecule chemically interacts with the substrate in its ground state without any excitations. This interaction alters the polarizability of the metal-molecule complex, leading to increased Raman cross-sections and variations in the shapes of the Raman spectra [68].

Secondly, the μ_{PICT} effect is wavelength-dependent and arises from CT between the substrate and a molecule in resonance with the incident photons. In a metal-molecule system, this CT can arise in either the molecule-to-metal or metal-to-molecule direction, depending on the relative positions of the Fermi level in the metal and HOMO/LUMO levels in the molecule (as depicted in Fig. 5c). The most significant PICT effect generally occurs when there is CT to or from levels near the metal's Fermi level. Additionally, resonance Raman scattering (RRS) can occur when the laser excitation frequency closely matches the electronic transition frequency of the molecule (μ_{mol}), contributing significantly, typically by a magnitude of 10^2 to 10^6, to the overall Raman signal strength. It is worth noting that RRS effects are particularly prominent in fluorescent molecules, although increased fluorescence is a significant drawback in such cases. It is important to mention that in non-metal substrates, additional CT transitions can similarly influence the enhancements in SERS. For instance, in semiconductors, exciton resonance can be involved, where electrons transfer from the VB to the CB, creating electron-hole pairs also called excitons (depicted in Fig. 5d). The CT mechanism in semiconductors is comparable to that in metal substrates but comprises a band gap that separates the VB and CB. The maximum SERS enhancement in semiconductors is typically observed at the band edges [69].

3. Technological advancements

Due to the growing urgency of developing flexible and reliable detection approaches for PFAS detection, many research groups have contributed to different sensors which can detect PFAS at low concentrations. Additionally, a SPR-based plastic optical fibre (POF) biosensor was developed to detect PFOS and PFOA in an aqueous solution. Cennamo et al. established a sensing platform used to determine the change in the resonance wavelength of PFOS and PFOA at concentrations ranging from 0 to 100 ppb (parts per billion) [70].

Despite the urgent need of ultrasensitive and rapid detection methods, only a few studies on the detection of PFAS using SERS have been published to till date. Fang and his co-workers used SERS techniques to detect firefighting foams, which are a major source of the PFAS fate in environmental concern [44]. There have been detections of PFOS, PFOA, and perfluorooctanesulfonic acid (6:2FTS). The LOD for PFOA is 50 ppb. Two SERS substrates were prepared using nanosphere lithography Ag and graphene oxide (GO) membrane to demonstrate the high loading affinity of the GO surface for fluoro surfactants (FS). Rather than straight loading FS on the SERS substrate surface, the dye-FS precipitate ion pair was loaded. Ethyl violet (EV) dye was used, and it behaves as a Raman probe because of its high Raman activity compared to FS. Two SERS substrates were prepared, dye-FS-Ag and dye-FS-GO, respectively, to detect FS. The FS was enhanced through the use of dye [44]. SEM images of SERS substrates are shown in Fig. 6. Fig. 6a shows the silica nanosphere embedded in a 200 nm thick Ag layer. The top and side views of the GO membrane taken at titling angle 30° are displayed in Fig. 6b and c, respectively. The SEM morphology of Ag NPs deposited on the GO membrane surface is shown in Fig. 6d.

The smooth surfaces of the incorporated Si-Ag-GO membranes allow the targeted PFAS compounds to adsorb rather than trap or embed. Fig. 6e-h illustrates the Raman spectra of dye-FS-Ag. The GO membrane in Fig. 6e was protected overnight in a solution of 5 ppm PFOA, 1 ppm EV, and 10 ppm sodium chloride (NaCl). Due to the significant improvement of the Raman signal on the Ag surface, Raman scattering on the GO surface should also be significantly enhanced, albeit not as significantly as on the Ag surface. In Fig. 6f and g, a controlled experiment was performed using the GO membrane (not the Ag surface) in a solution of 1 ppm EV with 10 mM NaCl (absence of FS) [44]. When associated with a dye, the typical peaks of EV were amplified (2–20-fold), supporting the proposition that the existence of a dye increases the loading capacity of FS onto the GO surface. Keeping in mind that the PFOA has been substituted by PFOS (Fig. 6f), and the 6:2 FTS has been replaced by 6:2FTS (Fig. 6g). Another substance was substituted in the ion-pair of dye–FS, the dye–from EV to MB to supplement the preceding statement. Fig. 6h illustrates the resulting finding. Fig. 6I and j illustrate dye-FS-Ag LOD assemblies. The dye-FS-GO LOD incubation assemblies are shown in Fig. 6k and l, respectively. Fig. 6l shows that the LOD should be 50 ppb, rather than the higher concentrations (50 and 5 ppb), where the Raman signal is stronger and more intense. When the GO membrane was relatively thin, the silicon peak at 512 cm^{-1} assisted as an internal reference [44].

Bai and coworkers fabricated plasmonic superstructure arrays and applied them for the detection of PFOA through SERS analysis [71]. PFOA is a strong fluorescent material, hence difficult to sense through the SERS technique. As PFOA is a fluorescent material, the fluorescence persuaded by the Raman excitation laser might screen Raman signals. One of the solutions is using longer Raman excitation wavelengths of 633 nm, which helps in suppress the fluorescence; though, this may diminish the Raman intensity due to the lower photon energy for general

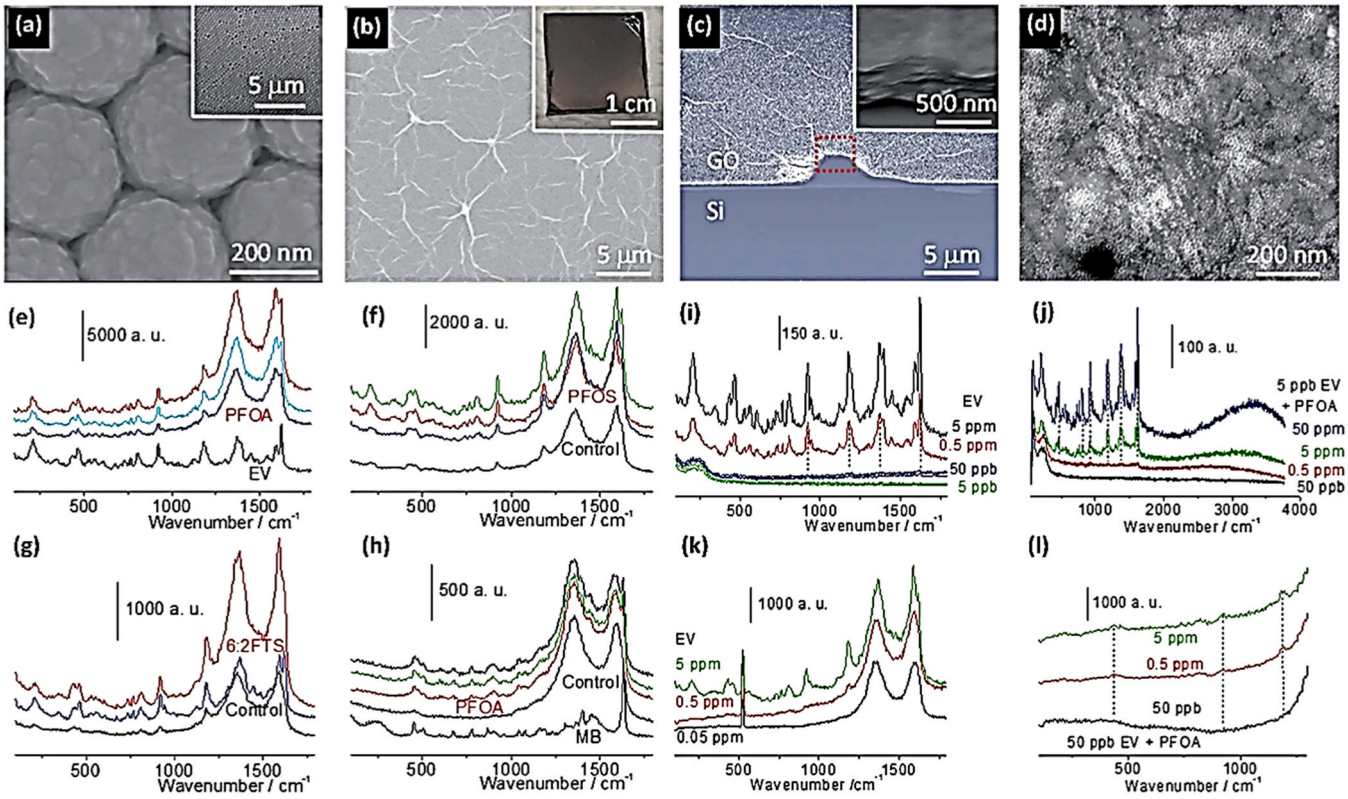

Fig. 6. SEM morphology of SERS substrate (a) displays the silica nanosphere surface coated with Ag nanoparticles; (b) and (c) shows that top-view and side-view of depicted GO membrane, (d) demonstrates that the Ag NPs deposited on the GO membrane; (e-h) shows that the Raman spectral analysis of the assemblage of dye–FS–GO; (k) and (l) shows the dye-FS-GO LOD incubation assemblies [44].

Ag nanoparticles [71]. As a result, laser near-field reduction tuned Ag plasmonic superstructure arrays with LSPR for the longer wavelength is useful for the wide-range studies of PFOA. Due to its LSPR at 657 nm, the plasmonic superstructure arrays with a 500 nm period used in this work were produced using a continuous wave (CW) laser. Although a hybrid superstructure of Au or Ag spherical nanoparticles can be produced using the laser near-field reduction approach, the hybrid structure's LSPR would be higher than 657 nm owing to the LSPR of Au. Because the Ag plasmonic superstructure's LSPR at 657 nm matches the employed Raman excitation wavelength (633 nm), it remained chosen for this measurement. Therefore, crystal violet (CV) was added to PFOA for Raman detection to prevent fluorescence [71]. When compared to the direct detection of PFOA, the incorporation of CV into PFOA significantly reduces the power of the Raman excitation laser and shortens the exposure time. This leads to the suppression of fluorescence generated by PFOA for precise sensing. The addition of PFOA to CV empowered the CV to display higher Raman activity through the development of ion-pairs among CV and PFOA. The produced ion pairs enhance the Raman activity and are useful for Raman measurements. This causes the number of analyte molecules adsorbed on the plasmonic superstructure arrays to increase. The fact that the creation of ion pairs did not cause the CV's Raman scattering wavenumber to change is another noteworthy observation [44].

Fig. 7a shows the SERS spectra of PFOA using a plasmonic hollow nanocluster array. For the baseline, 10^{-7} M of CV solution was used in this work. The Raman intensity gradually rises with the increase in concentration of PFOA owing to the formation of more ion-pairs with concentration. The LOD of PFOA can be determined as 3.3 σ/k, where σ

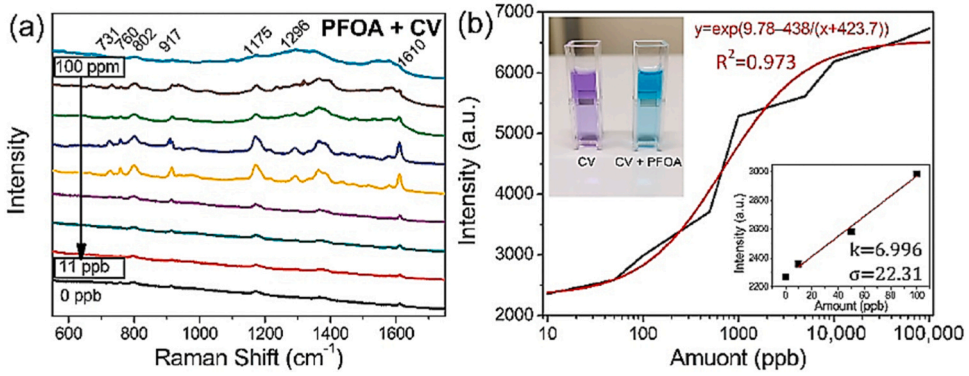

Fig. 7. SERS study of PFOA utilising a plasmonic hollow nanoclusters array. (a) SERS spectra of 10^{-7} M CV mixed with different concentrations of PFOA, measured using a plasmonic superstructure array with a period of 500 nm (b) The calibration curve for the sensing of PFOA for the Raman peak at 1175 cm^{-1} (inset photograph of CV solution (left) and CV mixed PFOA solution). [71].

represents the standard error of the y-intercept in the regression line and k stands for slope with respect to the IUPAC definition [72,73]. The LOD is determined in the lower concentration range of 0–100 ppb, which is 10.52 ppb according to this description of a linear relationship. When PFOA reached 100 ppm, two broad peaks related to its fluorescence were observed between 1000 and 1620 cm^{-1}; however, these overlapped with the Raman signals and were hence undetectable. As a result, the upper detection limit for PFOA, which is 100 ppm, cannot be reached with the current technology. For varying PFOA concentrations, Fig. 4b displays a calibration curve for the Raman intensity of CV with respect to 1175 cm^{-1}.

Since the fluorescence of PFOA at higher concentrations obscures the Raman peaks of CV, the fluorescence intensity is used to determine the upper detection limit for PFOA [71]. Therefore, compared to the 500 nm periodic superstructure, the 1000 nm periodic superstructure had a greater detection limit. Additionally, the author calculated how well PFOA could be detected when polyvinylpyrrolidone (PVP) was added. According to the data, PVP has a slight effect on the Raman signal's strength. However, only PFOA can raise the peak intensity of CV through the creation of ion pairs. As a result, the use of plasmonic superstructure arrays can enable the specific detection of PFOA through indirect analysis [71].

Fig. 8a shows the SERS spectra of PFOS surface integration onto Ag/graphene surface, with the spectrum from bulk source at the bottom and declining analyte concentrations (10^{-3} to 10^{-12} M) from bottom to top [74]. Additional peaks were observed and the source is unknown, but their presence could be ascribed to the SERS effect, which is the augmentation of vibrational modes that are otherwise not observable in standard Raman spectroscopy studies. The ability of the present SERS sensors to detect low quantities of PFOS is demonstrated by the persistence of the C-F peaks down to the lowermost PFOS concentration (10^{-12} M). The Raman and SERS spectra of PFOA are shown in Fig. 8b. The band from as-obtained powder is exposed at the bottom of Fig. 8b. PFOA has multiple similar peaks, such as the CF deformation mode of about 730 cm^{-1} and the CC stretching mode of about 1350 cm^{-1}. The PFOA concentration-dependent on SERS spectra (Fig. 8b) shows less stronger than those of PFOS. LOD of PFOS and PFOA obtained are 10^{-12} M and 10^{-9} M, respectively [74].

Huang and group have implemented SERS for analyzing PFAS [75]. To generate the LSPR effect required for SERS, 40 nm Ag NPs were employed. Utilizing the SERS approach, PFAS concentrations as detected down to 20 femto grams/liter in 30 s. A mixture of Ag NPs and water samples was prepared in a ratio of 2:3 and subsequently drop-casted onto aluminum substrates. The specific choice of 40 nm Ag NPs, which were kept at a temperature of 5 °C prior to usage, was made in order to fine-tune the enhancement of SERS. Aluminum foil was selected as the physical substrate to minimize any potential interference with the Raman signal. Raman spectra were obtained for PFAS and PFOA with Ag NPs with good enhancement. As a result, SERS has shown a significant improvement for both PFOA and PFOS. The Raman peak at 1300 cm^{-1} was recognized as the asymmetric stretching mode of the difluoro methylene (CF_2) group, which confirms the support of PFAS [75].

When PFAS sensors are fabricated from different types of materials, several limitations exist. Here are some of the key limitations and their associated details:

1. **Selectivity:** One of the major challenges in PFAS sensing is achieving high selectivity for target PFAS compounds. PFAS molecules can have similar structures and properties, making it difficult to differentiate between them accurately. Many sensor materials may exhibit cross-reactivity, leading to false-positive or false-negative results when detecting specific PFAS compounds [76].
2. **Sensitivity:** Another limitation is achieving high sensitivity in PFAS sensors. Due to the low concentrations of PFAS often found in environmental samples, sensors need to be highly sensitive to detect these compounds reliably. However, some sensor materials may not provide sufficient sensitivity, leading to lower detection limits and potential missed detections [77].
3. **Stability and Durability:** PFAS sensors should maintain their performance over extended periods. However, some materials used in sensor fabrication may exhibit limited stability and durability, especially when exposed to harsh environmental conditions or repeated use. Factors such as material degradation, fouling, or loss of sensitivity over time can affect the sensor's reliability and lifespan [78].
4. **Interference and Matrix Effects:** Environmental matrices often contain various interfering substances that can impact PFAS sensing. These interferences can affect the selectivity and sensitivity of the sensor, leading to inaccurate results. The presence of matrix effects, such as high ionic strength or complex sample matrices, can further complicate PFAS sensing and result in decreased sensor performance [79].
5. **Cost and Scalability:** The cost of materials used in PFAS sensors can influence their widespread deployment and accessibility. Some sensor materials may be expensive, limiting their practicality for large-scale monitoring applications. Additionally, the scalability of sensor fabrication processes can be challenging, impacting the availability and affordability of PFAS sensors [64,67,68,80].

Addressing these limitations requires ongoing research and

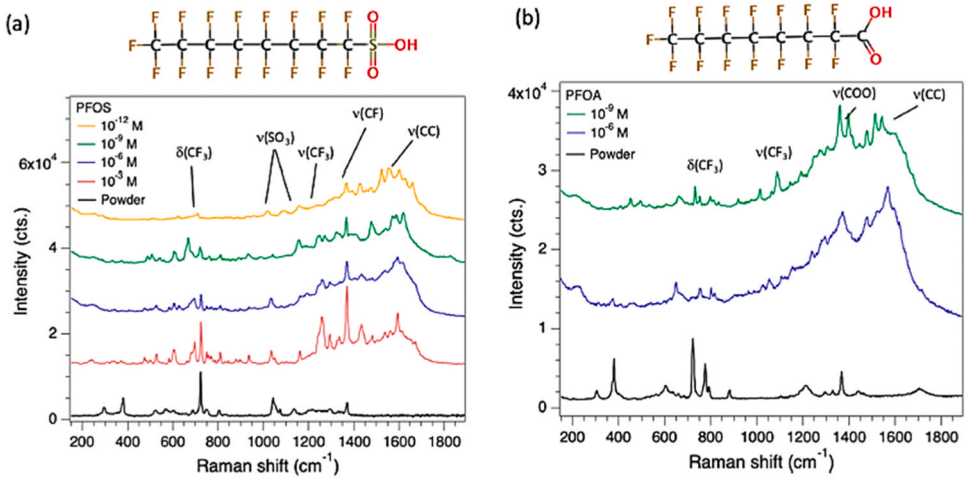

Fig. 8. Ag+graphene arrays were used for SERS detection of PFOS and PFOA. SERS of (a) PFOS and (b) PFOA under excitation at 633 nm. The structure of each molecule is displayed above the Raman spectra [74].

development efforts to improve the selectivity, sensitivity, stability, and cost-effectiveness of PFAS sensors. Integration of advanced materials, surface functionalization techniques, and signal processing algorithms are being explored to overcome these challenges and enhance the performance of PFAS sensing technologies. Table 2**.** Summarizes the available literature on the detection of PFAS via SERS and respective LOD. From these studies, it is confirmed that SERS is a highly effective technique for the detection of PFAS [44,71,74,75,81]. In recent days, the SERS technique is further extended to the detection of corona virus, amino acids, and drug molecules [82–84].

4. Fluorescence in Raman spectroscopy and methods to avoid

It is highly necessary to discuss the suppression of fluorescence in Raman scattering at this stage. Due to the strong fluorescence of PFAS, its detection is difficult and thus limited. Knowing the causes of the fluorescence in Raman scattering and how to address this issue are crucial from this viewpoint. As a result, fluorescence can be reduced and PFAS detection effectiveness can be increased. The presence of fluorescence alongside Raman spectra is one of the most significant concerns. This is due to the similar origins and strong competition between Raman scattering and fluorescence emission. In the majority of applications, the measured Raman spectrum is typically obscured by a high fluorescence background. This occurs because fluorescence emission is more potent than Raman scattering [85]. Two fundamental problems arise due to the fluorescence backdrop are removal of fluorescence causes errors in both concentration measurement and material identification since the Raman bands are narrow and the fluorescence has a smooth spectrum. Additionally, it reduces the signal-to-noise ratio by dominating the photon shot noise. This problem still causes restrictions on Raman applicability in some cases [48].

Raman scattering and fluorescence have some significant differences, which makes it easier to separate them. Raman scattering has a lifespan that is significantly shorter than fluorescence emission [86]. The fluorescence background will be greatly reduced, and the Raman signal will be significantly boosted when a molecule interacts with the metal nanoparticles. As a result, SERS has enhanced quickly [87–89]. Their discrepancies may contribute to a decrease in fluorescence and a consequent increase in Raman scattering.

Limitations and advantages of PFAS detection using fluorescence of Raman scattering.

Detection of PFAS using fluorescence of Raman scattering has both limitations and advantages.

Limitations of fluorescence-based detection of PFAS in Raman scattering: [71,74,75].

1. **Background Interference:** Fluorescence interference can be a significant limitation in fluorescence-based detection. Fluorescence from impurities or sample matrices can overlap with the Raman signal, leading to false-positive or false-negative results. This interference can hinder the accurate detection and quantification of PFAS [90].
2. **Signal-to-Noise Ratio:** Fluorescence signals can be relatively weak compared to background noise, especially in complex samples or at low analyte concentrations. The low signal-to-noise ratio can limit the sensitivity and reliability of the PFAS detection, making it challenging to detect trace levels of PFAS accurately [91].
3. **Overlapping Emission Spectra:** PFAS often exhibit fluorescence emission spectra that overlap with other fluorescent species present in the sample. This spectral overlap can make it difficult to distinguish and differentiate the fluorescence signals of PFAS from other interfering components, affecting the specificity and selectivity of the detection [92].
4. **Photobleaching:** Fluorescent molecules can undergo photobleaching, leading to a loss of fluorescence signal intensity over time. This degradation of fluorescence can limit the duration of measurements and the stability of the detection method [93].

Advantages of fluorescence-based detection of PFAS in Raman scattering:

1. **Enhanced sensitivity:** The combination of Raman scattering and fluorescence detection can provide enhanced sensitivity compared to conventional Raman spectroscopy. Fluorescence-based detection amplifies the weak Raman signals, making it possible to detect PFAS at lower concentrations and improve the limit of detection [94].
2. **Selectivity and specificity:** PFAS exhibit unique fluorescence spectra, allowing for their specific identification and differentiation from other fluorescent species. This selectivity and specificity can enable accurate detection and quantification of PFAS in complex samples containing multiple fluorescent components [95].
3. **Multiplexing capability:** Fluorescence-based detection allows for the simultaneous detection of multiple PFAS or other fluorescent analytes within a single measurement. By using different fluorophores or probes, multiple PFAS can be targeted and analyzed simultaneously, providing high-throughput capabilities [96].
4. **Imaging and visualization:** Fluorescence detection in Raman scattering can be utilized for imaging and visualization purposes. It allows the spatial distribution and localization of PFAS to be mapped in samples, providing valuable insights into their distribution and concentration gradients [97].
5. **Non-destructive analysis:** Fluorescence-based detection is non-destructive, allowing for repeated measurements on the same sample without altering its chemical or physical properties. This non-destructive nature facilitates the investigation of dynamic processes and longitudinal studies [98,99].

Overall, fluorescence-based detection of PFAS in Raman scattering offers enhanced sensitivity, selectivity, multiplexing capabilities, imaging possibilities, and non-destructive analysis. However, limitations related to background interference, signal-to-noise ratio, spectral overlap, and photobleaching should be considered when developing and applying this detection method. Careful experimental design, appropriate sample preparation, and advanced data analysis techniques can help mitigate these limitations and improve the accuracy and reliability of PFAS detection using fluorescence of Raman scattering. [100–105].

There are mainly three different ways to diminish the fluorescence.

1) Time-Domain Methods.

Ultra-short laser pulses are necessary for time-domain techniques [106]. On the timescale, where fluorescence has a substantially longer lifetime than Raman scattering (about hundreds of picoseconds to a few nanoseconds). This method takes advantage of the differences in response between the two signals (picoseconds to femtoseconds). The fast-arriving Raman scattered light could be temporally detached by an ultrafast optical pulse from the late- arriving fluorescence emission of a sample [48,107]. The temporal profiles of the excitation laser pulse, the

Table 2
Summarizes the available literature on the detection of PFAS via SERS and respective LOD.

SI No.	Material	PFAS	LOD	Laser Wavelength (nm)	Refrences
1	Ag NPs + Graphene oxide	PFOS PFOA	50 ppb	532	[44]
2	Ag NPs + Silica	PFOA	11–400ppb	405	[71]
3	Ag NPs + Graphene	PFOS PFOA	10^{-12} M 10^{-9} M	532 633	[74]
4	Ag NPs	PFOA PFOS	10^{-15} g/l	780	[75]

Raman scattering signal, and the fluorescence signal are shown in Fig. 9. The excitation laser light and the Raman emission occur almost simultaneously [107].

2) Frequency-Domain Methods.

This technique is also known as the phase-modulation technique. The Fourier transform relates time-domain and frequency-domain techniques [108]. This method contains two categories [109,110]. The frequency domain demodulation technique is based on the disparate responses of Raman scattering and fluorescence to high-frequency manipulation [109]. In Frequency-domain phase nulling, a function generator integrated into a gain-modulated image intensive produces sinusoidally modulated light at an angular frequency to illuminate the sample [111].

3) Wavelength-Domain Methods.

According to Kasha's theory, a fluorescence peak's wavelength does not considerably change with the excitation wavelength, whereas a Raman peak's wavelength closely tracks the excitation source's wavelength [112]. This idea is making use of wavelength-domain methods to reinforce tremendously weak Raman signals that are fluorescence-dominated while eliminating the fluorescence [113]. Shifted excitation Raman difference spectroscopy (SERDS), wavelength-modulated Raman spectroscopy (WMRS), and subtracted shifted Raman spectroscopy are typical wavelength-domain techniques (SSRS).

4) Computational Methods.

Computational techniques have been broadly used to post process measured Raman spectra directly to eliminate the fluorescence background, in addition to experimental techniques for fluorescence suppression. The wavelet transforms, derivatives, and polynomial fitting are the three most utilised computational techniques [114–116].

5) Other methods.

Other techniques for suppressing fluorescence emission exist, none of which fall under the categories mentioned above. Dark-field Raman microscopy [117], the polarisation modulation approach [118], Laguerre-Gaussian or holey-Gaussian beams [119], photobleaching [120] etc.

Challenges related to the detection of PFAS by the SERS method.

The detection of PFAS using the SERS method faces several challenges. These challenges include:

1. **Signal Enhancement:** While SERS provides significant signal enhancement, the detection of PFAS using SERS can be challenging due to their low Raman scattering cross-sections. PFAS molecules often exhibit weak Raman scattering signals, which can make it difficult to achieve sufficient signal enhancement for sensitive detection [121].
2. **Substrate Selection:** The choice of suitable SERS substrates for PFAS detection is crucial. PFAS molecules have unique chemical structures, and not all SERS-active substrates may interact effectively with PFAS, leading to weak or inconsistent signals. Developing specialized substrates that can effectively enhance the Raman signals of PFAS molecules is a challenge [122].
3. **Surface Adsorption and Aggregation:** PFAS tend to adsorb onto surfaces, including SERS substrates. This can lead to aggregation or clustering of PFAS molecules, altering their chemical environment and potentially affecting the Raman signals. Controlling the surface interactions and minimizing aggregation effects is important for accurate and reliable detection [123].
4. **Matrix Interference:** Environmental samples often contain complex matrices that can interfere with the detection of PFAS using SERS. Interfering substances may contribute to background signals or spectral overlap, making it challenging to distinguish the Raman signals of PFAS molecules from the background noise. Sample preparation techniques to reduce matrix interference and improve selectivity are necessary [124].
5. **Quantification:** Quantitative analysis of PFAS using SERS can be challenging due to the lack of suitable reference standards and calibration methods. Accurate quantification requires establishing a calibration curve using known concentrations of PFAS, which may be difficult due to the limited availability of PFAS standards and their often-complex mixture compositions [125–130].

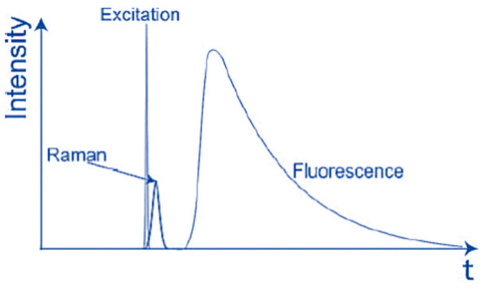

Fig. 9. Temporal profiles of the emitted fluorescence, emitted Raman scattering signal, and emitted laser excitation pulse. While the fluorescence intensity decreases exponentially over time, the Raman emission nearly immediately follows the excitation laser pulse [48].

5. Future research directions for PFAS detection via SERS

As observed from the literature, it is highly difficult to detect PFAS through SERS because of its high fluorescence. SERS is an extremely sensitive technique for the detection of analytes. SERS shows high sensitivity, excellent performance, and reproducibility, which are frequently cited as critical characteristics for analytical application analysis. Precise stages based on SERS nanotags, chemosensors, and chiral-selective systems have been developed and synthesized within this framework to support a variety of sensing strategies. As PFAS are highly fluorescent, their detection is challenging. It is observed that both fluorescence emission and Raman scattering have similar origins, and it is hence difficult to separate them. Many of the methods discussed above are of great importance in diminishing fluorescence. Different ways, such as time-domain, frequency-domain, wavelength-domain, computational, and other approaches, are briefly discussed. With these techniques, its detection efficiency can be enhanced.

The implementation of nanomaterials can significantly decrease fluorescence. As PFAS are soluble in water, their detection in water is essential. In this regard, the nanomaterials used for the detection of PFAS can be synthesized in water, which makes them facile for the real-time detection of PFAS. It is well known that anisotropic nanostructures have outstanding direction dependent properties, which makes them a very special class [131]. Highly faceted nanostructures with more edges and vertices are rich sources of hotspots and thus beneficial in the ultra-low detection of PFAS. This is because electromagnetic field distribution is more concentrated at edges and vertices than at faces [46]. Shape and size-dependent nanostructures (nanorods, nanocubes, octahedral, decahedral) were believed to show extraordinary enhancement due to different surface energies with various planes present in the anisotropic nanostructure. So, ultra-low detection of PFAS demands highly faceted anisotropic nanostructures. Core-shell or alloys of low-cost anisotropic nanostructures are assumed to show enhanced SERS due to synergistic effects [132]. Spiky nanostructures also exhibit a great improvement in signal enhancement due to their sharp tips [133]. Nanogap between nanostructures, which affects the detection limit. Nanogaps are rich in hotspots, and hence uniform distribution of hotspots brings a significant input to ultra-low detection of PFAS via SERS [134]. Uniform nanogaps can be achieved by the formation of an assembly of nanostructures [135]. Different assemblies like side-by-side, end-to-end, and bridging facets can create a uniform distribution of hotspots and thus help in the detection [45,136]. The selection of laser wavelength and power can also affect the detection of analytes in SERS. When the laser wavelength and nanostructure plasmon wavelength

match, that yields the best signal enhancement [137]. SERS is an extremely specific and selective technique for identifying the molecular fingerprint information of PFAS through Raman scattering without generating toxic waste. SERS is an excellent tool for multiple analyte detection, different PFAS can be analyzed simultaneously. One more important aspect of SERS is the detection of analytes in water. As water does not affect the Raman spectra [138], water-soluble PFAS can be detected in the solution form. Metal nanoparticles that interact with PFAS or PFAS functionalized with dye molecules, or thiol compounds can be enhanced many folds due to the creation of hotspots. The addition of external additives like dye molecules [12] has a certain limit of detection for PFOA; hence, fine tuning of detection methods is required without the addition of additives in order to detect PFOA at an ultra-low concentration. Ongoing research is being conducted to apply the SERS method to real-world samples. To enhance the accuracy of concentration calibration curves, the analysis of data will involve the integration of Partial Least Squares (PLS) regression along with genetic algorithm variable selection [75]. There are both advantages and disadvantages to fluorescence-based detection of PFAS in Raman scattering. Hence, the choice of parameters during the analysis can certainly help to improve the signal quality and intensity. There are some ways to diminish the fluorescence like Time-Domain Methods, Frequency-Domain Methods, Wavelength-Domain Methods, Computational Methods, and some other methods. All the above-mentioned parameters and inputs can be considered in future research directions to improve PFAS detection.

6. Conclusions

This perspective article focuses on the detection of one of the hazardous emerging contaminants, PFAS. The article gives a complete information related to PFAS, their hazardous effects, detection techniques, existing literature for detection via SERS and future outcomes to improve the detection efficiency. The article initially discusses the properties, uses, and hazardous effects of PFAS. Later on, traditional and current approaches for the detection of PFAS are discussed which include, chromatographic techniques combined with mass spectrometry, liquid chromatography solid-phase extraction, tandem mass spectrometry, optical, electrochemical, fluorescence-based sensors, and biosensors were also mentioned. From these methods, it is observed that PFOA and PFOS were only focused as an analyte for the detection. The LOD results achieved from these techniques are non-satisfactory and onsite detection is not possible. SERS stands as a great solution to overcome problems associated with these methods. The main two mechanisms of SERS: electromagnetic enhancement and chemical enhancement were discussed in detail. Even though SERS is sensitive and precise for detection, only a few literature are available. This is because of the difficulty in the detection of PFAS and the main problem with fluorescence. The limitations of PFAS sensors like selectivity, sensitivity, stability, durability, interference and matrix effects, and cost and scalability were also detailed. The article also discussed about the cause of fluorescence and the different methods to diminish fluorescence such as Computational Methods, Time-Domain Methods, Wavelength-Domain Methods, Frequency-Domain Methods, and other methods were mentioned. Fluorescence-based detection of PFAS in Raman scattering has both limitations and advantages, which are discussed in the article. Challenges related to the detection of PFAS by the SERS method is also one of the important section, deliberated here. Finally, all the possible future research directions and conclusions are given to further improvise the detection efficiency of PFAS via SERS.

CRediT authorship contribution statement

The perspective has been written through the contributions of all authors. All authors have approved the final version of the perspective.

Declaration of Competing Interest

The authors declare that they have no known competing financial interests or personal relationships that could have appeared to influence the work reported in this paper.

Data availability

No data was used for the research described in the article.

Acknowledgements

BMB acknowledges JAIN University for Junior Research Fellowship. AKS is grateful to the Science and Engineering Research Board (SERB), New Delhi, India (CRG/2018/003533), Karnataka Science and Technology Promotion Society Science and (KSTePS/VGST-RGS-F/2018–19/GRD No. 831/315), and JAIN University (JU/MRP/CNMS/16/2022) for the funding.

References

1 W.S. Dean, H.A. Adejumo, A. Caiati, P.M. Garay, A.S. Harmata, L. Li, E. E. Rodriguez, S. Sundar, A framework for regulation of new and existing PFAS by EPA, J. Sci. Policy Gov. 16 (2020) 1–14. ⟨https://www.sciencepolicyjournal.org/uploads/5/4/3/4/5434385/dean_adejumo_caiati_etal_jspg_v16.pdf⟩.
2 Z. Wang, J.C. DeWitt, C.P. Higgins, I.T. Cousins, A never-ending story of per-and polyfluoroalkyl substances (PFASs)? Environ. Sci. Technol. 51 (2017) 2508–2518, https://doi.org/10.1021/acs.est.6b04806.
3 L.J. Winchell, M.J. Wells, J.J. Ross, X. Fonoll, J.W. Norton Jr, S. Kuplicki, M. Khan, K.Y. Bell, Analyses of per-and polyfluoroalkyl substances (PFAS) through the urban water cycle: Toward achieving an integrated analytical workflow across aqueous, solid, and gaseous matrices in water and wastewater treatment, Sci. Total Environ. 774 (2021), 145257, https://doi.org/10.1016/j.scitotenv.2021.145257.
4 M.F. Rahman, S. Peldszus, W.B. Anderson, Behaviour and fate of perfluoroalkyl and polyfluoroalkyl substances (PFASs) in drinking water treatment: a review, Water Res. 50 (2014) 318–340, https://doi.org/10.1016/j.watres.2013.10.045.
5 C. Hogue, How to say goodbye to PFAS, Chem. Eng. N. 97 (2019) 22–25. ⟨https://www.cheric.org/research/tech/periodicals/view.php?seq=1782808⟩.
6 C.C. Bach, B.H. Bech, N. Brix, E.A. Nohr, J.P.E. Bonde, T.B. Henriksen, Perfluoroalkyl and polyfluoroalkyl substances and human fetal growth: a systematic review, Crit. Rev. Toxicol. 45 (2015) 53–67, https://doi.org/10.3109/10408444.2014.952400.
7 A. Kärrman, K. Elgh-Dalgren, C. Lafossas, T. Møskeland, Environmental levels and distribution of structural isomers of perfluoroalkyl acids after aqueous fire-fighting foam (AFFF) contamination, Environ. Chem. 8 (2011) 372–380, https://doi.org/10.1071/EN10145.
8 R. Naidu, M. Bowman, 4th International Contaminated Site Remediation Conference. Adelaide, South Australia A23, 2012.
9 R.C. Buck, J. Franklin, U. Berger, J.M. Conder, I.T. Cousins, P. De Voogt, A. A. Jensen, K. Kannan, S.A. Mabury, S.P. van Leeuwen, Perfluoroalkyl and polyfluoroalkyl substances in the environment: terminology, classification, and origins, Integ. Environ. Assess. Manag. 7 (2011) 513–541, https://doi.org/10.1002/ieam.258.
10 Z. Wang, I.T. Cousins, M. Scheringer, R.C. Buck, K. Hungerbühler, Global emission inventories for C4–C14 perfluoroalkyl carboxylic acid (PFCA) homologues from 1951 to 2030, Part I: production and emissions from quantifiable sources, Environ. Int. 70 (2014) 62–75, https://doi.org/10.1016/j.envint.2014.04.013.
11 K. Prevedouros, I.T. Cousins, R.C. Buck, S.H. Korzeniowski, Sources, fate and transport of perfluorocarboxylates, Environ. Sci. Technol. 40 (2006) 32–44, https://doi.org/10.1021/es0512475.
12 C. Fang, R. Dharmarajan, M. Megharaj, R. Naidu, Gold nanoparticle-based optical sensors for selected anionic contaminants, TrAC 86 (2017) 143–154, https://doi.org/10.1016/j.trac.2016.10.008.
13 S.R. Fenton, A. Ducatman, A. Boobis, J.C. DeWitt, C. Lau, C. Ng, S.M. Roberts, Per-and polyfluoroalkyl substance toxicity and human health review: Current state of knowledge and strategies for informing future research, Environ. Toxicol. Chem. 40 (2021) 606–630, https://doi.org/10.1002/etc.4890.
14 United States Environmental Protection Agency, EPA's fifth Unregulated Contaminant Monitoring Rule (UCMR 5). ⟨https://www.epa.gov/sdwa/questions-and-answers-drinking-water-health-advisories-pfoa-pfos-genx-chemicals-and-pfbs⟩.
15 J.L. Domingo, M. Nadal, Human exposure to per-and polyfluoroalkyl substances (PFAS) through drinking water: a review of the recent scientific literature, Environ. Res. 177 (2019), 108648, https://doi.org/10.1016/j.envres.2019.108648.
16 A.L. Hagstrom, P. Anastas, A. Boissevain, A. Borrel, N.C. Deziel, S.E. Fenton, C. Fields, J.D. Fortner, N. Franceschi-Hofmann, R. Frigon, Yale School of Public Health Symposium: an overview of the challenges and opportunities associated with per-and polyfluoroalkyl substances (PFAS), Sci. Total Environ. 778 (2021), 146192, https://doi.org/10.1016/j.scitotenv.2021.146192.
17 L. Rosenblum, S. Wendelken, Method 533: determination of per-and polyfluoroalkyl substances in drinking water by isotope dilution anion exchange

solid phase extraction and liquid chromatography/tandem mass spectrometry, Tandem Mass Spectrom. 52 (2019).
18 J. Shoemaker, D. Tettenhorst, Method 537.1: determination of selected per-and polyfluorinated alkyl substances in drinking water by solid phase extraction and liquid chromatography/tandem mass spectrometry (LC/MS/MS), National Center for Environmental Assessment, Washington, DC, 2018.
19 R.F. Menger, E. Funk, C.S. Henry, T. Borch, Sensors for detecting per-and polyfluoroalkyl substances (PFAS): A critical review of development challenges, current sensors, and commercialization obstacles, J. Chem. Eng. 417 (2021), 129133, https://doi.org/10.1016/j.cej.2021.129133.
20 T. Groffen, L. Bervoets, Y. Jeong, T. Willems, M. Eens, E. Prinsen, A rapid method for the detection and quantification of legacy and emerging per-and polyfluoroalkyl substances (PFAS) in bird feathers using UPLC-MS/MS, J. Chromatogr. B 1172 (2021), 122653, https://doi.org/10.1016/j.jchromb.2021.122653.
21 H. Ryu, B. Li, S. De Guise, J. McCutcheon, Y. Lei, Recent progress in the detection of emerging contaminants PFAS, J. Hazard. Mater. 408 (2021), 124437, https://doi.org/10.1016/j.jhazmat.2020.124437.
22 K.L. Rodriguez, J.H. Hwang, A.R. Esfahani, A.A. Sadmani, W.H. Lee, Recent developments of PFAS-detecting sensors and future direction: a review, Micromachines 11 (2020) 667, https://doi.org/10.3390/mi11070667.
23 H. Chen, X. Wang, C. Zhang, R. Sun, J. Han, G. Han, X. He, Occurrence and inputs of perfluoroalkyl substances (PFASs) from rivers and drain outlets to the Bohai Sea, China, Environ. Pollut. 221 (2017) 234–243, https://doi.org/10.1016/j.envpol.2016.11.070.
24 H. Lin, J. Niu, D. Ding, L. Zhang, Electrochemical degradation of perfluorooctanoic acid (PFOA) by Ti/SnO2–Sb, Ti/SnO2–Sb/PbO2 and Ti/SnO2–Sb/MnO2 anodes, Water Res. 46 (2012) 2281–2289, https://doi.org/10.1016/j.watres.2012.01.053.
25 T.D. Appleman, E.R. Dickenson, C. Bellona, C.P. Higgins, Nanofiltration and granular activated carbon treatment of perfluoroalkyl acids, J. Hazard. Mater. 260 (2013) 740–746, https://doi.org/10.1016/j.jhazmat.2013.06.033.
26 J.L. Guelfo, C.P. Higgins, Subsurface transport potential of perfluoroalkyl acids at aqueous film-forming foam (AFFF)-impacted sites, Environ. Sci. Technol. 47 (2013) 4164–4171, https://doi.org/10.1021/es3048043.
27 Y.C. Chen, S.L. Lo, J. Kuo, Effects of titanate nanotubes synthesized by a microwave hydrothermal method on photocatalytic decomposition of perfluorooctanoic acid, Water Res. 45 (2011) 4131–4140, https://doi.org/10.1016/j.watres.2011.05.020.
28 X. Chen, X. Xia, X. Wang, J. Qiao, H. Chen, A comparative study on sorption of perfluorooctane sulfonate (PFOS) by chars, ash and carbon nanotubes, Chemosphere 83 (2011) 1313–1319, https://doi.org/10.1016/j.chemosphere.2011.04.018.
29 Y.C. Lee, P.Y. Wang, S.L. Lo, C.P. Huang, Recovery of perfluorooctane sulfonate (PFOS) and perfluorooctanoate (PFOA) from dilute water solution by foam flotation, Sep. Purif. Technol. 173 (2017) 280–285, https://doi.org/10.1016/j.seppur.2016.09.012.
30 A. Papadopoulou, I.P. Román, A. Canals, K. Tyrovola, E. Psillakis, Fast screening of perfluorooctane sulfonate in water using vortex-assisted liquid–liquid microextraction coupled to liquid chromatography–mass spectrometry, Anal. Chim. Acta 691 (2011) 56–61, https://doi.org/10.1016/j.aca.2011.02.043.
31 J.G. Sepulvado, A.C. Blaine, L.S. Hundal, C.P. Higgins, Occurrence and fate of perfluorochemicals in soil following the land application of municipal biosolids, Environ. Sci. Technol. 45 (2011) 8106–8112, https://doi.org/10.1021/es103903d.
32 S. Takagi, F. Adachi, K. Miyano, Y. Koizumi, H. Tanaka, M. Mimura, K. Kannan, Perfluorooctanesulfonate and perfluorooctanoate in raw and treated tap water from Osaka, Japan, Chemosphere 72 (2008) 1409–1412, https://doi.org/10.1016/j.chemosphere.2008.05.034.
33 E.M. Sunderland, X.C. Hu, C. Dassuncao, A.K. Tokranov, C.C. Wagner, J.G. Allen, A review of the pathways of human exposure to poly- and perfluoroalkyl substances (PFASs) and present understanding of health effects, J. Expo. Sci. Environ. Epidemiol. 29 (2019) 131–147, https://doi.org/10.1038/s41370-018-0094-1.
34 W.M.A. Niessen, A.P. Tinke, Liquid chromatography-mass spectrometry general principles and instrumentation, J. Chromatog. A 703 (1995) 37–57, https://doi.org/10.1016/0021-9673(94)01198-N.
35 H. Park, J. Park, W. Kim, W. Kim, J. Park, Ultra-sensitive SERS detection of perfluorooctanoic acid based on self-assembled p-phenylenediamine nanoparticle complex, J. Hazard. Mater. 453 (2023), 131384, https://doi.org/10.1016/j.jhazmat.2023.131384.
36 V. skandari, H. Sahbafar, L. Zeinalizad, F. Sabzian-Molaei, M.H. Abbas, A. Hadi, surface-enhanced Raman scattering (SERS) biosensor fabricated using the electrodeposition method for ultrasensitive detection of amino acid histidine, J. Mol. Struct. 1274 (2023), 134497, https://doi.org/10.1016/j.molstruc.2022.134497.
37 S.X. Leong, Y.X. Leong, E.X. Tan, H.Y.F. Sim, C.S.L. Koh, Y.H. Lee, X.Y. Ling, Noninvasive and point-of-care surface-enhanced Raman scattering (SERS)-based breathalyzer for mass screening of coronavirus disease 2019 (COVID-19) under 5 min, ACS nano 16 (2022) 2629–2639, https://doi.org/10.1021/acsnano.1c09371.
38 J.R. Ferraro, Introductory raman spectroscopy, Elsevier, 2003. ⟨https://www.google.co.in/books/edition/Introductory_Raman_Spectroscopy/9_s-XBnLcMcC?hl=en&gbpv=0⟩.
39 J. Zhu, Q. Chen, F.Y. Kutsanedzie, M. Yang, Q. Ouyang, H. Jiang, Highly sensitive and label-free determination of thiram residue using surface-enhanced Raman spectroscopy (SERS) coupled with paper-based microfluidics, Anal. Methods 43 (2017) 6186–6193, https://doi.org/10.1039/C7AY01637A.
40 B.L. Sanchez-Gaytan, P. Swanglap, T.J. Lamkin, R.J. Hickey, Z. Fakhraai, S. Link, S.-J. Park, Spiky gold nanoshells: synthesis and enhanced scattering properties, J. Phys. Chem. C. 116 (2012) 10318–10324, https://doi.org/10.1021/jp300009b.
41 K. Kneipp, H. Kneipp, R. Manoharan, I. Itzkan, R.R. Dasari, M.S. Feld, Near-infrared surface-enhanced Raman scattering can detect single molecules and observe 'hot' vibrational transitions, J. Raman Spectrosc. 29 (1998) 743–747, https://doi.org/10.1002/(SICI)1097-4555(199808)29:8%3C743::AID-JRS294%3E3.0.CO;2-M.
42 J. Jiang, K. Bosnick, M. Maillard, L. Brus, Single molecule Raman spectroscopy at the junctions of large Ag nanocrystals, J. Phys. Chem. B. 107 (2003) 9964–9972, https://doi.org/10.1021/jp034632u.
43 J. Langer, D. Jimenez de Aberasturi, J. Aizpurua, R.A. Alvarez-Puebla, B. Auguié, J. J. Baumberg, G.C. Bazan, S.E. Bell, A. Boisen, A.G. Brolo, Present and future of surface-enhanced Raman scattering, ACS NANO 14 (2019) 28–117, https://doi.org/10.1021/acsnano.9b04224.
44 C. Fang, M. Megharaj, R. Naidu, Surface-enhanced Raman scattering (SERS) detection of fluorosurfactants in firefighting foams, RSC Adv. 6 (2016) 11140–11145, https://doi.org/10.1039/C5RA26114G.
45 M.B. Bhavya, S.R. Manippady, M. Saxena, B. Ramya Prabhu, N.S. John, R. G. Balakrishna, A.K. Samal, Gold Nanorods as an efficient substrate for the detection and degradation of pesticides, Langmuir 36 (2020) 7332–7344, https://doi.org/10.1021/acs.langmuir.0c00809.
46 M.B. Bhavya, B. Ramya Prabhu, B.M. Shenoy, P. Bhol, S. Swain, M. Saxena, N. S. John, G. Hegde, A.K. Samal, Femtomolar detection of thiram via SERS using silver nanocubes as an efficient substrate, Environ. Sci. Nano 7 (2020) 3999–4009, https://doi.org/10.1039/D0EN01049A.
47 H. Wei, S.M.H. Abtahi, P.J. Vikesland, Plasmonic colorimetric and SERS sensors for environmental analysis, Environ. Sci. Nano 2 (2015) 120–135, https://doi.org/10.1039/C4EN00211C.
48 D. Wei, S. Chen, Q. Liu, Review of fluorescence suppression techniques in Raman spectroscopy, Appl. Spectrosc. Rev. 50 (2015) 387–406, https://doi.org/10.1080/05704928.2014.999936.
49 M.B. Bhavya, B. Ramya Prabhu, A. Tripathi, G. Hegde, N.S. John, R. Thapa, G. Hegde, R.G. Balakrishna, M. Saxena, A. Altaee, A.K. Samal, Functionalized Silver Nanocubes for the Detection of Hazardous Analytes through SERS: Experimental and Computational Studies, ACS Sustain, Chem. Eng. (2023), https://doi.org/10.1021/acssuschemeng.3c00069.
50 Y. Zhang, X. Zhang, Surface-enhanced Raman scattering for detection and analysis of perfluoroalkyl substances: A review, TrAC 127 (2020), 115892.
51 S. Lee, S. Choi, S. Park, Surface-enhanced Raman spectroscopy for the analysis of per- and polyfluoroalkyl substances: A review, Anal. Chim. Acta 1079 (2019) 1–15.
52 B. Sharma, R.R. Frontiera, A.I. Henry, E. Ringe, SERS: Materials, applications, and the future, Mater. Today 15 (2012) 16–25, https://doi.org/10.1016/S1369-7021(12)70017-2.
53 V. Langer, J. Dahlen, L. Malmqvist, C. Östman, Raman spectroscopy for identification and quantification of perfluorinated compounds in environmental matrices. Environ. Sci. Process, Impacts 19 (2017) 401–408.
54 X.-M. Qian, S.M. Nie, Single-molecule and single-nanoparticle SERS: from fundamental mechanisms to biomedical applications, Chem. Soc. Rev. 37 (2008) 912–920, https://doi.org/10.1039/B708839F.
55 S. Fateixa, H.I. Nogueira, T. Trindade, Hybrid nanostructures for SERS: materials development and chemical detection, Phys. Chem. Chem. Phys. 17 (2015) 21046–21071, https://doi.org/10.1039/C5CP01032B.
56 D.-Y. Wu, X.-M. Liu, S. Duan, X. Xu, B. Ren, S.-H. Lin, Z.-Q. Tian, Chemical enhancement effects in SERS spectra: A quantum chemical study of pyridine interacting with copper, silver, gold and platinum metals, J. Phys. Chem. C. 112 (2008) 4195–4204, https://doi.org/10.1021/jp0760962.
57 W. Ren, C. Zhu, E. Wang, Enhanced sensitivity of a direct SERS technique for Hg 2+ detection based on the investigation of the interaction between silver nanoparticles and mercury ions, Nanoscale 4 (2012) 5902–5909, https://doi.org/10.1039/C2NR31410J.
58 L. Jensen, C.M. Aikens, G.C. Schatz, Electronic structure methods for studying surface-enhanced Raman scattering, Chem. Soc. Rev. 37 (2008) 1061–1073, https://doi.org/10.1039/B706023H.
59 G. McNay, D. Eustace, W.E. Smith, K. Faulds, D. Graham, Surface-enhanced Raman scattering (SERS) and surface-enhanced resonance Raman scattering (SERRS): a review of applications, Appl. Spect. 65 (2011) 825–837, https://doi.org/10.1366/11-06365.
60 K.A. Willets, R.P. Van Duyne, Localized surface plasmon resonance spectroscopy and sensing, Annu. Rev. Phys. Chem. 58 (2007) 267–297, https://doi.org/10.1146/annurev.physchem.58.032806.104607.
61 B. Sharma, R.R. Frontiera, A.-I. Henry, E. Ringe, R.P. Van Duyne, SERS: Materials, applications, and the future, Mater. Today 15 (2012) 16–25, https://doi.org/10.1016/S1369-7021(12)70017-2.
62 X. Wang, W. Shi, G. She, L. Mu, Surface-Enhanced Raman Scattering (SERS) on transition metal and semiconductor nanostructures, Phys. Chem. Chem. Phys. 14 (2012) 5891–5901, https://doi.org/10.1039/c2cp40080d.
63 J.R. Lombardi Alessandri, Enhanced Raman scattering with dielectrics, Chem. Rev. 116 (2016) 14921–14981, https://doi.org/10.1021/acs.chemrev.6b00365.
64 Y. Kim, N.J. Jang, H. Kim, G.C. Kim, Y. Yi, S.Yoon Shin, Study of chemical enhancement mechanism in non-plasmonic surface enhanced Raman spectroscopy (SERS), Front. Chem. 7 (2019) 582, https://doi.org/10.3389/fchem.2019.00582.
65 H.K. Lee, Y.H. Lee, C.S.L. Koh, G.C. Phan-Quang, X. Han, C.L. Lay, H.Y.F. Sim, Y. C. Kao, Q. An, X.Y. Ling, Designing surface-enhanced Raman scattering (SERS) platforms beyond hotspot engineering: emerging opportunities in analyte manipulations and hybrid materials, Chem. Soc. Rev. 48 (2019) 731–756, https://doi.org/10.1039/C7CS00786H.
66 S. Cong, X. Liu, Y. Jiang, W. Zhang, Z. Zhao, Surface enhanced Raman scattering revealed by interfacial charge-transfer transitions, Innovation 1 (2020) 3, https://doi.org/10.1016/j.xinn.2020.100051.

67 E. Petryayeva, U.J. Krull, Localized surface plasmon resonance: nanostructures, bioassays and biosensing-a review, Anal. Chim. Acta 706 (2011) 8–24, https://doi.org/10.1016/j.aca.2011.08.020.
68 C.M. Jensen, G.C. Schatz Aikens, Electronic structure methods for studying surface-enhanced Raman scattering, Chem. Soc. Rev. 37 (2008) 1061–1073, https://doi.org/10.1039/B706023H.
69 J.R. Lombardi, R.L. Birke, Theory of surface-enhanced Raman scattering in semiconductors, J. Phys. Chem. C. 118 (2014) 11120–11130, https://doi.org/10.1021/jp5020675.
70 N. Cennamo, G. D'Agostino, G. Porto, A. Biasiolo, C. Perri, F. Arcadio, L. Zeni, A molecularly imprinted polymer on a plasmonic plastic optical fiber to detect perfluorinated compounds in water, Sensors 18 (2018) 1836, https://doi.org/10.3390/s18061836.
71 S. Bai, A. Hu, Y. Hu, Y. Ma, K. Obata, K. Sugioka, Plasmonic superstructure arrays fabricated by laser near-field reduction for wide-range SERS analysis of fluorescent materials, Nanomaterials 12 (2022) 970, https://doi.org/10.3390/nano12060970.
72 M.-M. Huang, L.-N. Xu, Construction of a new luminescent Cd (ii) compound for the detection of Fe3+ and treatment of Hepatitis B, Open Chem. 19 (2021) 953–960, https://doi.org/10.1515/chem-2021-0085.
73 A. Haider, M. Ahmed, M. Faisal, M.M. Naseer, Isatin as a simple, highly selective and sensitive colorimetric sensor for fluoride anion, Heterocycl. Commun. 26 (2020) 14–19, https://doi.org/10.1515/hc-2020-0003.
74 A. McDonnell, F.M. Albarghouthi, R. Selhorst, N. Kelley-Loughnane, A.D. Franklin, R. Rao, Aerosol Jet Printed Surface-Enhanced Raman Substrates: Application for High-Sensitivity Detection of Perfluoroalkyl Substances, ACS Omega 8 (2022) 1597–1605, https://doi.org/10.1021/acsomega.2c07134.
75 T. Huang, A. McClelland, T.H. Zeng, Trace PFAS detection in water sources using silver nanoparticles for surface-enhanced Raman spectroscopy (SERS), 2022 IEEE 22nd Int. Conf. Nanotechnol. (2022) 342–345, https://doi.org/10.1109/NANO54668.2022.9928684.
76 X. Tao, S. Yu, R. Ji, L. Chen, Recent advances in sensing techniques for perfluorinated compounds, TrAC 139 (2021), 116324.
77 Y. Gao, Q. Hu, S. Luo, X. Cai, Y. Huang, Advances in the detection of perfluoroalkyl acids and their precursors: A review, Environ. Pollut. 251 (2019) 471–481.
78 Y. Wang, H. Xu, J. Yan, H. Yu, W. Hu, Recent advances in sensors for per- and polyfluoroalkyl substances (PFASs) detection: A review. Trends Environ, Anal. Chem. 29 (2021), e00111.
79 X. Liu, M. Li, H. Jin, H. Chen, Emerging trends in sensing techniques for per- and polyfluoroalkyl substances (PFASs): A review, TrAC 125 (2020), 115860.
80 D. Di Palma, M. Rivas, M.P. Gallardo, Marco, Strategies and challenges for the detection of per- and polyfluoroalkyl substances (PFAS) in water, Water Res. 202 (2021), 117396.
81 T. Huang, A. McClelland, T.H. Zeng, Trace PFAS Detection in Water Sources Using Silver Nanoparticles for Surface-Enhanced Raman Spectroscopy (SERS), 2022 IEEE 22nd Int. Conf. Nanotechnol. (2022) 342–345, https://doi.org/10.1109/NANO54668.2022.9928684.
82 S.X. Leong, Y.X. Leong, E.X. Tan, H.Y.F. Sim, C.S.L. Koh, Y.H. Lee, C. Chong, L. S. Ng, J.R.T. Chen, D.W.C. Pang, L.B.T. Nguyen, Noninvasive and point-of-care surface-enhanced Raman scattering (SERS)-based breathalyzer for mass screening of coronavirus disease 2019 (COVID-19) under 5 min, ACS nano 16 (2022) 2629–2639, https://doi.org/10.1021/acsnano.1c09371.
83 V. Eskandari, H. Sahbafar, L. Zeinalizad, F. Sabzian-Molaei, M.H. Abbas, A. Hadi, A surface-enhanced Raman scattering (SERS) biosensor fabricated using the electrodeposition method for ultrasensitive detection of amino acid histidine, J. Mol. Struct. 1274 (2023), 134497, https://doi.org/10.1016/j.molstruc.2022.134497.
84 V. Eskandari, H. Sahbafar, L. Zeinalizad, R. Mahmoudi, F. Karimpour, A. Hadi, H. Bardania, Coating of silver nanoparticles (AgNPs) on glass fibers by a chemical method as plasmonic surface-enhanced Raman spectroscopy (SERS) sensors to detect molecular vibrations of Doxorubicin (DOX) drug in blood plasma, Arab. J. Chem. 15 (2022), 104005, https://doi.org/10.1016/j.arabjc.2022.104005.
85 P. Matousek, M. Towrie, C. Ma, W.M. Kwok, D. Phillips, W. Toner, A. Parker, Fluorescence suppression in resonance Raman spectroscopy using a high-performance picosecond Kerr gate, J. Raman Spectrosc. 32 (2001) 983–988, https://doi.org/10.1002/jrs.784.
86 F. Ariese, H. Meuzelaar, M.M. Kerssens, J.B. Buijs, C. Gooijer, Picosecond Raman spectroscopy with a fast intensified CCD camera for depth analysis of diffusely scattering media, Analyst 134 (2009) 1192–1197, https://doi.org/10.1039/B821437A.
87 C. Yuen, Q. Liu, Towards in vivo intradermal surface enhanced Raman scattering (SERS) measurements: silver coated microneedle based SERS probe, Wiley Online Libr. 7 (2014) 683–689, https://doi.org/10.1002/jbio.201300006.
88 A. Campion, P. Kambhampati, Surface-enhanced Raman scattering, Chem. Soc. Rev. 27 (1998) 241–250, https://doi.org/10.1039/A827241Z.
89 F. Dong, J. Ye, S. Hu, A.T. Popov, M. Friberg, Muhammed, Fluorescence quenching and photobleaching in Au/Rh6G nanoassemblies: impact of competition between radiative and non-radiative decay, J. Eur. Opt. Soc. Rapid Publ. 6 (2011), https://doi.org/10.2971/jeos.2011.11019.
90 Y. Wang, J. Yan, H. Xu, H. Yu, W. Hu, A high-throughput method for analysis of per- and polyfluoroalkyl substances in environmental waters using direct injection and online solid-phase extraction coupled to liquid chromatography-tandem mass spectrometry, J. Chromatogr. A 1627 (2020), 461387.
91 L. Naidoo, E. Chimuka, Cukrowska, Analytical methods for the determination of per- and polyfluoroalkyl substances (PFASs) in environmental matrices: A review, Anal. Bioanal. Chem. 410 (2018) 3571–3593.
92 Y. Shi, Q. Zhou, J. Hu, Q. Zhang, Y. Zhao, G. Jiang, Review on the analytical methods for determination of perfluorinated compounds in environmental samples, Environ. Res. 126 (2013) 56–80.
93 X. Gao, Y. Cui, R.M. Levenson, L.W. Chung, S. Nie, In vivo cancer targeting and imaging with semiconductor quantum dots, Nat. Biotechnol. 22 (2004) 969–976. ⟨https://www.nature.com/articles/nbt994⟩.
94 C. Zong, M. Xu, L.J. Xu, X. Wei, H.W. Li, Recent advances in Raman spectroscopy for detecting biomarkers of diseases in blood and urine, J. Transl. Med 16 (2018) 1–20, https://doi.org/10.1021/acs.chemrev.7b00668.
95 T. Zhang, H. Sun, Q. Li, H. Xu, Y. Lv, Y. Sun, Y. Zhang, Progress and perspectives on the detection of perfluoroalkyl substances: A review, Anal. Chim. Acta 1081 (2019) 1–19.
96 H. Sun, Y. Tang, Q. Li, T. Zhang, H. Zhang, Y. Zhang, Recent advances in the analysis of per- and polyfluoroalkyl substances (PFASs) in environmental samples: A review, Anal. Chim. Acta 1110 (2020) 54–72.
97 Q. Li, T. Zhang, H. Sun, Y. Lv, Y. Sun, Y. Zhang, H. Xu, Progress in fluorescence-based imaging of per- and polyfluoroalkyl substances (PFASs): Principles, methods, and applications, Anal. Chim. Acta 1176 (2021), 338669.
98 Y. Zhao, H. Qian, X. Zhang, Nondestructive identification of intracellular poly-γ-glutamic acid (γ-PGA) using Raman and fluorescence spectra for rapid screening of high γ-PGA-producing strains, Sci. Rep. 6 (2016) 30314.
99 A.O. De Silva, et al., "Advances in the analysis of per- and polyfluoroalkyl substances in environmental samples.&quot, Environ. Sci.: Process. amp; Impacts 20 (2018) 30–54, https://doi.org/10.1039/c7em00482f.
100 J. Glüge, M. Scheringer, I.T. Cousins, J.C. DeWitt, G. Goldenman, D. Herzke, Z. Wang, An overview of the uses of per-and polyfluoroalkyl substances (PFAS), Environ. Sci.: Process. Impacts 22 (2020) 2345–2373, https://doi.org/10.1039/D0EM00291G.
101 J.L. Domingo, M. Nadal, Per-and polyfluoroalkyl substances (PFASs) in food and human dietary intake: a review of the recent scientific literature, J. Agric. Food Chem. 65 (2017) 533–543, https://doi.org/10.1021/acs.jafc.9b01449.
102 R. Vitorino, A.S. Barros, A. Caseiro, R. Ferreira, F. Amado, Evaluation of different extraction procedures for salivary peptide analysis, Talanta 94 (2012) 209–215, https://doi.org/10.1016/j.talanta.2012.03.023.
103 S. Kanan, F. Samara, Dioxins and furans: A review from chemical and environmental perspectives, Trends Environ. Anal. Chem. 17 (2018) 1–13, https://doi.org/10.1016/j.teac.2017.12.001.
104 K. Kannan, S. Corsolini, J. Falandysz, G. Fillmann, K.S. Kumar, K.S., B. G. Loganathan, K.M. Aldous, Perfluorooctanesulfonate and related fluorochemicals in human blood from several countries, Environ. Sci. Technol. 38 (2004) 4489–4495, https://doi.org/10.1021/es0493446.
105 Q. Lin, J. Wu, X. Fang, J. Kong, Washing-free centrifugal microchip fluorescence immunoassay for rapid and point-of-care detection of protein, Anal. Chim. Acta 1118 (2020) 18–25, https://doi.org/10.1016/j.aca.2020.04.031.
106 S.K. Sahoo, S. Umapathy, A.W. Parker, Time-resolved resonance Raman spectroscopy: Exploring reactive intermediates, Appl. Spectrosc. 65 (2011) 1087–1115, https://doi.org/10.1366/11-06406.
107 W. Becker, Fluorescence lifetime imaging–techniques and applications, J. Microsc. 247 (2012) 119–136, https://doi.org/10.1111/j.1365-2818.2012.03618.x.
108 A.Z. Genack, Electro-optic phase-sensitive detection of optical emission and scattering, Appl. Phy. Lett. 46 (1985) 341–343, https://doi.org/10.1063/1.95917.
109 F.V. Bright, G.M. Hieftje, A new technique for the elimination of fluorescence interference in Raman spectroscopy, Appl. Spectrosc. 40 (1986) 583–587. ⟨https://opg.optica.org/as/abstract.cfm?URI=as-40-5-583⟩.
110 M. Wirth, S.H. Chou, Comparison of time and frequency domain methods for rejecting fluorescence from Raman spectra, Anal. Chem. 60 (1988) 1882–1886, https://doi.org/10.1021/ac00169a009.
111 A. Genack, Fluorescence suppression by phase-resolved modulation Raman scattering, Anal. Chem. 56 (1984) 2957–2960, https://doi.org/10.1021/ac00278a075.
112 M. Kasha, Characterization of electronic transitions in complex molecules, Discuss. Faraday Soc. 9 (1950) 14–19, https://doi.org/10.1039/DF9500900014.
113 S.T. McCain, R.M. Willett, D.J. Brady, Multi-excitation Raman spectroscopy technique for fluorescence rejection, Opt. Express 16 (2008) 10975–10991, https://doi.org/10.1364/OE.16.010975.
114 V. Mazet, C. Carteret, D. Brie, J. Idier, B. Humbert, Background removal from spectra by designing and minimising a non-quadratic cost function, Chemom. Intell. Lab. Syst. 76 (2005) 121–133, https://doi.org/10.1016/j.chemolab.2004.10.003.
115 M. Ramos, I. Ruisánchez, Noise and background removal in Raman spectra of ancient pigments using wavelet transform, J. Raman Spectrosc.: Int. J. Orig. Work all Asp. Raman Spectrosc., Incl. High. Order Process., also Brillouin Rayleigh Scatt. 36 (2005) 848–856, https://doi.org/10.1002/jrs.1370.
116 M.N. Leger, A.G. Ryder, Comparison of derivative preprocessing and automated polynomial baseline correction method for classification and quantification of narcotics in solid mixtures, Appl. Spectrosc. 60 (2006) 182–193. ⟨https://opg.optica.org/as/abstract.cfm?URI=as-60-2-182⟩.
117 M.V. Schulmerich, R. Reddy, A.K. Kodali, L.J. Elgass, K. Tangella, R. Bhargava, Dark field Raman microscopy, Anal. Chem. 82 (2010) 6273–6280, https://doi.org/10.1021/ac1014194.
118 R.L. McCreery, Raman Spectroscopy for Chemical Analysis, John Wiley & Sons,, 2005. ⟨https://books.google.co.in/books?hl=en&lr=&id=qY4MI0Zln1YC&oi=fnd&pg=PR5&dq=118.%09R.+L.+McCreery,+Raman+spectroscopy+for+chemical+analysis,+John+Wiley+%26+Sons2005.&ots=ne5ixP2V3J&sig=RFT3zxFc4wN6unDxTmmpdkW3mBE&redir_esc=y#v=onepage&q&f=false⟩.

119 G. Cormack, M. Mazilu, K. Dholakia, C.S. Herrington, Fluorescence suppression within Raman spectroscopy using annular beam excitation, Appl. Phys. Lett. 91 (2007), 023903, https://doi.org/10.1063/1.2756311.

120 H. Hamaguchi, T. Tahara, M. Tasumi, Suppression of luminescence background in Raman spectroscopy by means of transient optical depletion of causal impurity molecules, Appl. Spectrosc. 41 (1987) 1265–1268. ⟨https://opg.optica.org/as/abstract.cfm?URI=as-41-8-1265⟩.

121 X. Ma, L. Yu, Surface-enhanced Raman spectroscopy for the analysis of perfluorooctanoic acid in environmental samples: A review. Trends in Environ, Anal. Chem. 22 (2019), e00075.

122 H. Wang, M. Zhang, X. Wang, P. Xu, Y. Ding, J. Zhan, Surface-enhanced Raman spectroscopy for the detection of perfluorooctane sulfonate (PFOS) in environmental samples: A review, Talanta 216 (2020), 120975.

123 H. Xie, Y. Liu, S. Liu, Z. Zhou, Y. Lu, Y. Yin, Recent advances in surface-enhanced Raman spectroscopy for the detection of per- and polyfluoroalkyl substances, Anal. Chim. Acta 1184 (2021), 339119.

124 X. Wang, S. Huang, M. Li, Recent advances in surface-enhanced Raman spectroscopy for the detection of per- and polyfluoroalkyl substances in complex environmental samples. TrAC Trends in, Anal. Chem. 139 (2020), 117425.

125 S. Chen, L. Yu, L. Chen, Surface-enhanced Raman spectroscopy for the analysis of perfluorinated compounds: Recent advances and future perspectives. Trends in Environ, Anal. Chem. 27 (2020), e00088.

126 M. Al Amin, Z. Sobhani, Y. Liu, R. Dharmaraja, S. Chadalavada, R. Naidu, C. Fang, Recent advances in the analysis of per-and polyfluoroalkyl substances (PFAS)—A review, Environ. Tech. Innov. 19 (2020), 100879, https://doi.org/10.1016/j.eti.2020.100879.

127 J. Jahn, O. Žukovskaja, X.S. Zheng, K. Weber, T.W. Bocklitz, D. Cialla-May, J. Popp, Surface-enhanced Raman spectroscopy and microfluidic platforms: challenges, solutions and potential applications, Analyst 142 (2017) 1022–1047, https://doi.org/10.1039/C7AN00118E.

128 Piotrowski, Surface-enhanced Raman scattering (SERS)-based detection of ions, 2017. ⟨https://depotuw.ceon.pl/handle/item/2452⟩.

129 C. Chen, W. Liu, S. Tian, T. Hong, Novel surface-enhanced Raman spectroscopy techniques for DNA, protein and drug detection, Sensors 19 (2019) 1712, https://doi.org/10.3390/s19071712.

130 T. Ong, E.W. Blanch, O.A. Jones, Surface Enhanced Raman Spectroscopy in environmental analysis, monitoring and assessment, Sci. Total Environ. 720 (2020), 137601, https://doi.org/10.1016/j.scitotenv.2020.137601.

131 T. Meincke, R.N.K. Taylor, Continuous flow synthesis of plasmonic gold patches and nearly-complete nanoshells on polystyrene core particles, Particuology 75 (2023) 137–150, https://doi.org/10.1016/j.partic.2022.06.007.

132 X. Liu, J. Ma, P. Jiang, J. Shen, R. Wang, Y. Wang, G. Tu, Large-scale flexible surface-enhanced Raman scattering (SERS) sensors with high stability and signal homogeneity, ACS Appl. Mater. Interfaces 12 (2020) 45332–45341, https://doi.org/10.1021/acsami.0c13691.

133 Z. Huang, G. Meng, X. Hu, Q. Pan, D. Huo, H. Zhou, Y. Ke, N. Wu, Plasmon-tunable Au@Ag core-shell spiky nanoparticles for surface-enhanced Raman scattering, Nano Res. 12 (2019) 449–455, https://doi.org/10.1007/s12274-018-2238-y.

134 L. Tong, H. Xu, M. Käll, Nanogaps for SERS applications, Mrs Bull. 39 (2014) 163–168, https://doi.org/10.1557/mrs.2014.2.

135 A. Fahes, A. En Naciri, M. Navvabpour, S. Jradi, S. Akil, Self-assembled Ag nanocomposites into ultra-sensitive and reproducible large-area SERS-Active opaque substrates, Nanomaterials 11 (2021) 2055, https://doi.org/10.3390/nano11082055.

136 M.B. Bhavya, B. Ramya Prabhu, A. Tripathi, S. Yadav, N.S. John, R. Thapa, A. Altaee, M. Saxena, A.K. Samal, A unique bridging facet assembly of gold nanorods for the detection of thiram through surface-enhanced Raman scattering, ACS Sustain. Chem. Eng. 10 (2022) 7330–7340, https://doi.org/10.1021/acssuschemeng.2c01089.

137 D.K. Medipally, A. Maguire, J. Bryant, J. Armstrong, M. Dunne, M. Finn, F.M. Lyng, A.D. Meade, Development of a high throughput (HT) Raman spectroscopy method for rapid screening of liquid blood plasma from prostate cancer patients, Analyst 142 (2017) 1216–1226, https://doi.org/10.1039/C6AN02100J.

138 L. Chen, S. Guo, L. Dong, F. Zhang, R. Gao, Y. Liu, Y. Wang, Y. Zhang, SERS effect on the presence and absence of rGO for Ag@Cu2O core-shell, Mater. Sci. Semicond. Process. 91 (2019) 290–295, https://doi.org/10.1016/j.mssp.2018.11.038.